Remote Sensing of Environment 171 (2015) 218–233

Contents lists available at ScienceDirect

Remote Sensing of Environment

journal homepage: www.elsevier.com/locate/rse

A rule-based approach for mapping macrophyte communities using multi-temporal aquatic vegetation indices

Paolo Villa [a,*], Mariano Bresciani [a], Rossano Bolpagni [b], Monica Pinardi [a,b], Claudia Giardino [a]

[a] Institute for Electromagnetic Sensing of the Environment, National Research Council (IREA-CNR), Milan, Italy
[b] Department of Life Sciences, University of Parma (UNIPR), Parma, Italy

ARTICLE INFO

Article history:
Received 15 May 2015
Received in revised form 17 September 2015
Accepted 22 October 2015
Available online 2 November 2015

Keywords:
Aquatic plants
Functional groups
Shallow lakes
Classification
Classification Tree (CT)
NDVI
NDAVI
WAVI
Landsat 7 ETM+
Landsat 8 OLI
ALOS AVNIR-2

ABSTRACT

Macrophytes are important components of freshwater ecosystems, playing a relevant role in carbon and nutrient cycles. Notwithstanding their widespread diffusion in temperate to subtropical shallow lakes, little effort has been performed so far in extensively mapping macrophyte communities at regional to continental scale. A rule-based classification scheme was implemented for mapping four macrophyte community types (helophyte, emergent rhizophyte, floating, and submerged-floating association). Input features were selected among multi-spectral reflectance and multi-temporal vegetation indices, based on Landsat data acquired over four test sites: Lake Taihu (China), Kis-Balaton wetland (Hungary), Lake Trasimeno and Mantua Lakes system (Italy). The best performing features were derived from Water Adjusted Vegetation Index (WAVI) computed at: early spring, maximum growth, and late autumn conditions. Overall accuracy (OA) and Kappa coefficient (k) of macrophyte maps produced with our approach over the ensemble of four sites were 90.1% and 0.865, respectively, with best performance in European temperate areas (OA = 93.6–94.2%, k = 0.887–0.916), and lower scores for subtropical Lake Taihu (OA = 82.8%, k = 0.762). Per-class accuracies were higher than 80% for all target classes, except for the submerged-floating association, with misclassifications concentrated in Taihu site. The robustness of the approach was tested over two independent validation cases: a different site (i.e. Lake Varese, Italy), and a different input dataset (i.e. AVNIR-2 data, for Mantua Lakes system). Consistent accuracy results were achieved: OA = 94.3% (k = 0.922) and OA = 85.6% (k = 0.766), with some misclassification due to spatial resolution of AVNIR-2 data.

1. Introduction

Macrophytes are important components of inland freshwater ecosystems (Jeppensen et al., 1997), playing a relevant role in the global carbon (e.g. gas fluxes, interactions with phytoplankton productivity) and nutrient (e.g. denitrification in sediments, nitrogen uptake) cycles (Wetzel, 1992; Jordan, Stoffer, & Nestlerode, 2011; Bolpagni et al., 2014), as well as in the provision of suitable niches for nursery and feeding activities for several aquatic faunal species and threatened taxa (e.g. amphibians, water birds and fish) (Schriver, Bogestrand, Jeppensen, & Sondergaard, 1995). All the more so, these roles could be further modified in the short term by the effects of the global change (Carmichael, Bernhardt, Brauer, & Smith, 2014; Jacobs & Harrison, 2014). Even if many evidences suggest an ambiguous role of climate warming on macrophytes, increments in growth rates and spatial distribution, as well as a general reinforcement of water eutrophication symptoms are expected (McKee et al., 2002; Kosten et al., 2011). This is especially true for shallow lakes and wetlands, in temperate to high latitude regions (Poff, Brinson, & Day, 2002; Dudgeon et al., 2006; Finlayson, Davis, Gell, Kingsford, & Parton, 2013).

As the Millennium Ecosystem Assessment (2005) has thoroughly assessed, in the last decades worldwide littoral lacustrine environments have experienced a dramatic reduction in extent and a sensible decline in water quality and functionality (e.g. Hicks & Frost, 2011; Bresciani, Bolpagni, Braga, Oggioni, & Giardino, 2012; Azzella, Rosati, Iberite, Bolpagni, & Blasi, 2014a). Water use and abuse for multiple human purposes, shoreline modification and reinforcement, and urban settlements development have heavily contributed to jeopardize the survival of riparian and littoral aquatic plant communities (Schmieder, 2004; Jeppesen et al., 2010).

Recent studies on marine coastal vegetated ecosystems (e.g. seagrasses, mangroves, salt marshes) have assessed both intensity and efficiency of carbon (C) fixation in vegetation and sediments and gave origin to the concept of the so called 'blue carbon' (Duarte, Middelburg, & Caraco, 2005; Mcleod et al., 2011; Duarte, Losada, Hendriks, Mazarrasa, & Marbà, 2013), relevant at global scale assessment of C budget. Concerning the terrestrial compartment, Abril et al. (2013) have demonstrated that flooded forests and wetlands play a crucial role in C fixation in the Amazon Basin. For inland freshwater ecosystems, the quantitative role of macrophytes communities in C cycle has

* Corresponding author at: via Bassini 15, 20133 Milan, Italy.
E-mail address: villa.p@irea.cnr.it (P. Villa).

http://dx.doi.org/10.1016/j.rse.2015.10.020
0034-4257/

been so far neglected, mainly due to the high spatial resolution needed to assess such processes from remote. Still, their role in terrestrial C cycling could be relevant, at least at watershed scale (Pinardi, Bartoli, Longhi, & Viaroli, 2011; Abril et al., 2013). Despite all this, little effort has been performed so far in extensively mapping aquatic vegetation cover and characteristics especially in shallow lakes, focusing on robust approaches to assess morpho-ecological gradients, structural complexity and functional status of macrophyte dominated habitats (Bolpagni et al., 2007; Ribaudo, Bartoli, Racchetti, Longhi, & Viaroli, 2011; Jacobs & Harrison, 2014). Macrophytes display a higher level of species diversity in temperate areas than in tropical ones, contrary to what happens for terrestrial plants (Crow, 1993), and show some cosmopolitan features, with 60% of known species being present on more than one continent (Sculthorpe, 1967); these two characteristics make macrophytes a very interesting target from regional to cross-continental studies at synoptic scale. Due to its repeatability and spatial coverage, Earth Observation (EO) can be considered an ideal tool to make large-scale inventories of wetland and aquatic vegetation communities across different ecosystems, and has long demonstrated theoretical capabilities and operational potential for such application (e.g. Penuelas, Gamon, Griffin, & Field, 1993; Caloz & Collet, 1997; Silva, Costa, Melack, & Novo, 2008; Xie, Sha, & Yu, 2008; Adam, Mutanga, & Rugege, 2010; Zlinszky, Mücke, Lehner, Briese, & Pfeifer, 2012; Klemas, 2013; Birk & Ecke, 2014). Tough, systematic, regional to global scale vegetation monitoring base on EO has been historically biased towards terrestrial vegetation, the main reason being that the vast majority of spectral vegetation analysis techniques have been designed on terrestrial vegetation (e.g. Carlson & Ripley, 1997; Pettorelli et al., 2005; Gray & Song, 2012; Yang, Weisberg, & Bristow, 2012). Moreover, most of the literature on macrophyte remote sensing focuses on the use of hyperspectral information (e.g., Williams, Rybicki, Lombana, O'Brien, & Gomez, 2003; Artigas & Yang, 2005; Giardino, Bartoli, Candiani, Pellegrini, & Bresciani, 2007; Hestir et al., 2008; Hunter, Gilvear, Tyler, Willby, & Kelly, 2010) or use multispectral imagery over limited targets, mostly consisting of a single study area (e.g. Munyati, 2000; Liira, Feldmann, Mäemets, & Peterson, 2010; Tian, Yu, Zimmerman, Flint, & Waldron, 2010; Albright & Ode, 2011; Dronova et al., 2012; Shuchman, Sayers, & Brooks, 2013), thus not completely assessing the capabilities of EO providing synoptic regional sampling with regular, operational data acquisitions. An exception is the work of Nelson, Cheruvelil, and Soranno (2006), that have used Landsat data to map four macrophyte groups in 13 small lakes with relatively low turbidity, all located in Michigan, U.S.; although they reached satisfying to good results over lakes used for model development (58–97% per-class concordance), when they validated the model over different lakes the mapping accuracy was drastically reduced (18–36% per-class concordance), failing to extend their approach to lakes not sampled in their training set.

The high discrimination capabilities demonstrated through the use of hyperspectral data is in fact balanced by the relatively high cost and low availability of such type of remote data, either from aerial or satellite platforms (e.g. Schaepman et al., 2009; Ben-Dor, Schlapfer, Plaza, & Malthus, 2013). Great potential in vegetation mapping applications has been shown by exploiting multi-temporal information, e.g. for assessing wetland vegetation in tidal marsh environments (e.g. Gilmore et al., 2008) and regularly flooded systems (e.g. Wang et al., 2012), as well as for mapping vegetation damage recovery patterns after extreme events (e.g. Villa, Boschetti, Morse, & Politte, 2012). The straightforwardness of spectral vegetation indices (VIs) has long demonstrated its advantages for large scale mapping of dynamic phenomena in both terrestrial (e.g. Huete, Justice, & Liu, 1994; Lunetta, Knight, Ediriwickrema, Lyon, & Worthy, 2006; Wardlow & Egbert, 2008) and aquatic environments (e.g. Hu, 2009; Hu et al., 2010; Villa, Duan, & Loiselle, 2015). In particular, Wang et al. (2012) showed capabilities and performance of temporal series of vegetation indices in mapping wetland vegetation groups on a functional basis over Lake Poyang, China, but more testing over different areas and cases need to be performed to reach consistent results beyond local, site-specific approaches.

The high spatial heterogeneity of macrophytes and their presence in relatively small water bodies and wetland areas, especially throughout temperate climates, needs to be monitored at a spatial resolution which is not supported by a majority of operational low resolution EO platforms (300–1000 m ground resolution) currently used for terrestrial vegetation applications at global scale (e.g. Fensholt & Proud, 2012; Brown, De Beurs, & Marshall, 2012; Liu, Dijk, McCabe, Evans, & Jeu, 2013; Hmimina et al., 2013). For this scope, medium resolution EO data (10–30 m ground resolution) is the best option in terms of balance between operational capabilities, large area coverage and spatial resolution for macrophyte monitoring applications that aim to go beyond the local scale with enough potential for detection capabilities from regional to global scales, and offers best capabilities when used for multivariate analysis in spectral and temporal domain (e.g. Villa, Lechi, & Gomarasca, 2009). Recently, spectral VIs specifically optimized for aquatic vegetation have been designed and tested using broadband spectral ranges currently available for an extended group of medium resolution EO sensors: i.e. the Normalized Difference Aquatic Vegetation Index (NDAVI, Villa, Laini, Bresciani, & Bolpagni, 2013; Villa, Mousivand, & Bresciani, 2014a) and the Water Adjusted Vegetation Index (WAVI; Villa et al., 2014a). Even if not as spectrally powerful as hyperspectral based one, a multispectral medium resolution mapping approach is at the moment showing the highest degree of flexibility and applicability in the context of macrophytes monitoring applications that aim to go beyond the local scale, as many applications in macrophyte analysis require (Farmer & Adams, 1989; Vis, Hudon, & Carignan, 2003). In this work, we re-adapted the functional group scheme proposed by Lacoul and Freedman (2006) for delineating four target macrophyte community types to be mapped, which are globally widespread and representative of temperate to subtropical environments: helophyte, emergent rhizophyte, floating (both free-floating and floating-leaved species), and submerged-floating association (i.e. the coexistence of floating and submerged species). We then assessed the efficiency of aquatic vegetation indices (NDAVI and WAVI) in capturing specific multi-temporal features of such community types. Based on this assessment, we eventually delivered a comprehensive rule-based approach for mapping macrophyte community types, relying on multi-temporal medium resolution data over a set of heterogeneous test and validation sites.

In this context, our study covers three main objectives, dealing with: i) assessing the performance of multi-spectral information compared to multi-temporal VIs and selecting the best VI for discriminating different macrophyte community classes; ii) exploiting the most efficient multi-temporal features for implementing a rule-based macrophyte community type mapping approach, and iii) validating the results derived from such approach over independent data and sites.

2. Test sites and rationale

We developed and tested our approach for macrophyte community types classification on five shallow water systems (average depth ranging from 2 to 11 m), featuring abundant and variegate macrophyte vegetation: Lake Taihu (eastern China), Kis-Balaton wetland (western Hungary), Lake Trasimeno (central Italy), Mantua Lakes system and Lake Varese (northern Italy). The five sites are located in the northern hemisphere and represent a gradient of environmental conditions, ranging from continental (including perialpine and Mediterranean regions) to subtropical climates, as well as limnological characteristics, from small, artificial wetlands to large hypertrophic lakes (Fig. 1).

Lake Taihu (central-eastern China; 31°14′ N, 120°12′ E), located in subtropical Yangtze Delta, is the third largest Chinese lake (surface of 2338 km^2; mean depth of ~2 m). The lake is subjected to severe eutrophication and suffers from massive cyanobacteria blooms in summer-autumn seasons since at least three decades, mainly as a result of industrial development and urbanization (Ning, Pan, Chen, & Liu, 2013). The

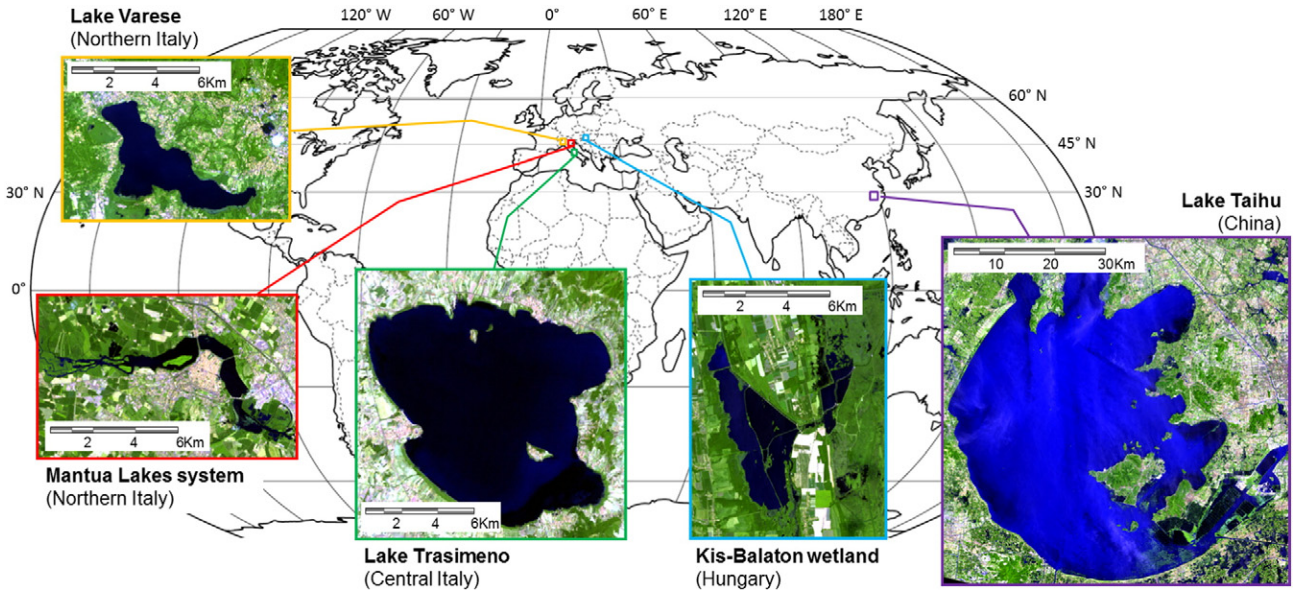

Fig. 1. Study areas overview, showing each of the five test sites (Lake Varese used only for validation) in RGB = 874 OLI band composition (scale varies with each case).

shoreline is largely colonized by *Phragmites australis* (Common reed), whereas the south-eastern part of the water body is dominated by dense stands of *Nymphoides peltata* (Yellow floating heart), *Trapa bicornis* (Asian water chestnut), *Potamogeton malaianus* (Bamboo-leaved pondweed), and *Vallisneria spiralis* (Coiled eelgrass) (Liu et al., 2007; Zhao et al., 2012).

Kis-Balaton (Hungary; 46°38′ N, 17°08′ E) is a large wetland (~81 km^2) located south-west of Lake Balaton, at the mouth of the Zala River. Drainage of the area began in the 18th century to broaden arable fields, and reshaping took place in the late 1970s making it a large constructed wetland, acting as buffer zone for the water inflow entering Lake Balaton (Zlinszky, 2010; Zlinszky & Timár, 2013). Since 1992, large sectors of the original water body (~51 km^2, max depth 2 m) were flooded again to recreate extensive Common reed and Sedge (*Carex* ssp.) meadows, with *Typha angustifolia* (lesser bulrush) intrusions. Water bodies are eutrophic and densely colonized by *Nuphar lutea* (Spatterdock), *Nymphaea alba* (Water lily), *Trapa natans* (Water chestnut), and *Ceratophyllum demersum* (Common hornwort) stands (Dinka et al., 2008; Zlinszky et al., 2012). During late summer, along the lake shores and in small canals and ponds of the area, *Lemna minor* (Common duckweed) often forms dense free-floating colonies, often in association with *Spirodela polyrrhiza* (Greater duckweed).

Lake Trasimeno (central Italy; 43°08′ N, 12°06′ E) is a roughly circular meso-eutrophic basin, both fluvial and tectonic in origin, and is the fourth largest lake in Italy (area of 124 km^2). It is a closed, un-stratified basin with depth not exceeding 6 m. Due to its shallowness, the lake is densely colonized by submerged macrophytes, especially in south-eastern part: e.g. by *Myriophyllum spicatum* (Eurasian water-milfoil), *Potamogeton perfoliatus* (Perfoliate pondweed), and *C. demersum*. Most spread emergent species along the shoreline are *P. australis*, *T. angustifolia*, and *Carex* ssp. (Giardino et al., 2015).

Mantua Lakes system (45°10′ N, 10°47′ E) and Lake Varese (45°48′ N, 8°44′ E) are located in Lombardy region (northern Italy). The Mantua Lakes system is composed by four small and shallow (average depth ~3.5 m) fluvial lakes and wetlands (total area of ~6 km^2) that surround the city of Mantua. The system is fed by the Mincio River (emissary of the Lake Garda) and exhibits a hypertrophic status and elevated sedimentation rates of organic matter (Pinardi et al., 2011). Waters are dominated by dense stands of *Nelumbo nucifera* (Lotus flower), *N. lutea*, and *T. natans*; the shorelines are mainly colonized by *P. australis* (Tomaselli, Gualmini, & Spettoli, 2000). Similar to Kis-Balaton, in late August the littoral zones are often colonized by dense free-floating stands of *L. minor*, *S. polyrrhiza* and *Salvinia natans* (Floating fern). Lake Varese is a monomictic basin with average depth of 11 m and a surface of ~15 km^2. The lake is eutrophic and characterized by moderate to high turbid conditions. Lake area, particularly along the southern part, is dominated by dense stands of *N. alba*, *T. natans*, with some *C. demersum*, whereas the riparian zones are dominated by *P. australis* (Azzella, Bolpagni, & Oggioni, 2014b).

For defining macrophyte mapping targets, we started from the basic functional groups proposed by Lacoul and Freedman (2006) for the non-arborescent aquatic and wetland plants (mostly angiosperms), that identifies four main groups: emergent (mostly helophytes), floating-leaved, free-floating, and submerged plant species (Cook, 1990). In order to follow more closely the morphological traits of some macrophyte communities (e.g. by taking into account different plant canopy height above water for such species as *N. lutea* and *N. nucifera*) we slightly re-adapted the scheme. We therefore specified distinct subtypes with respect to their interaction level with the water–atmosphere interface, thus distinguishing six detailed functional groups: i) helophyte, ii) emergent rhizophyte, iii) floating-leaved rhizophyte, iv) free-floating pleustophyte, v) submerged rhizophyte, and vi) submerged pleustophyte (see Table 1). This detailed functional group scheme can easily represent the vast majority of macrophyte growth forms and encompass the main aquatic vegetation typologies that can be recognized over large heterogeneous areas worldwide. Unlike terrestrial vegetation, which exhibits marked biogeographical patterning, aquatic plants are generally showing more cosmopolitan structural community features, even at the global scale (Crow, 1993; Chambers, Lacoul, Murphy, & Thomaz, 2008). Moving from the riparian to the inner parts of a water body, three distinct vegetation belts are generally recognized: a marginal strip dominated by helophytes, a littoral strip dominated by emergent, floating-leaved, and submerged rhizophytes, as well as by free-floating and submerged pleustophytes, and a pelagic strip dominated by submerged forms (both pleustophytes and rhizophytes). Table 1 summarizes the variability and representativeness of the functional group scheme with reference to our test sites.

Being based on optical response of aquatic vegetation from EO data with specific spectral and spatial characteristics, our macrophyte classification scheme must take into account the capabilities of satellite input data in capturing macrophyte heterogeneity levels. For example, discriminating floating-leaved rhizophyte from free-floating pleustophyte species is virtually impossible from multi-spectral satellite data at medium spatial resolution (10–30 m). Moreover, water column properties may severely affect the detectability of submerged species using optical

Table 1
Macrophytes functional groups and main species present in the study areas (the most relevant species for each site are underlined); *Car_ssp = Carex ssp*; *Cer_dem = Ceratophyllum demersum*; *Lem_min = Lemna minor*; *Myr_spi = Myriophyllum spicatum*; *Naj_mar = Najas marina*; *Nel_nuc = Nelumbo nucifera*; *Nup_lut = Nuphar lutea*; *Nym_alb = Nymphaea alba*; *Nym_pel = Nymphoides peltata*; *Phr_aus = Phragmites australis*; *Pot_cri = Potamogeton crispus*; *Pot_luc = Potamogeton lucens*; *Pot_mal = Potamogeton malaianus*; *Pot_nat = Potamogeton natans*; *Pot_per = Potamogeton perfoliatus*; *Sal_nat = Salvinia natans*; *Spi_pol = Spirodela polyrrhiza*; *Typ_ang = Typha angustifolia*; *Tra_bic = Trapa bicornis*; *Tra_nat = Trapa natans*; *Utr_vul = Utricularia vulgaris*; *Val_spi = Vallisneria spiralis*).

Macrophyte functional group	Lake Taihu	Kis-Balaton wetland	Lake Trasimeno	Mantua Lakes system	Lake Varese
Helophyte	*Phr_aus*	*Car_ssp* *Phr_aus* *Typ_ang*	*Car_ssp* *Phr_aus* *Typ_ang*	*Phr_aus*	*Phr_aus*
Emergent rhizophyte	–	–	–	*Nel_nuc*	–
Floating-leaved rhizophyte	*Nym_pel* *Tra_bic*	*Nym_alb* *Nup_lut* *Tra_nat*	–	*Nym_alb* *Nup_lut* *Tra_nat*	*Nym_alb* *Tra_nat*
Free-floating pleustophyte	–	*Lem_min* *Spi_pol*	–	*Lem_min* *Sal_nat* *Spi_pol*	–
Submerged rhizophyte	*Pot_mal* *Val_spi*	*Naj_mar*	*Myr_spi* *Naj_mar* *Pot_cri* *Pot_luc* *Pot_per*	*Naj_mar* *Val_spi*	*Naj_mar*
Submerged pleustophyte	*Cer_dem*	*Cer_dem* *Utr_vul*	*Cer_dem*	*Cer_dem*	*Cer_dem*

data, especially in turbid systems (such as the majority of shallow lakes and wetlands), where aquatic plants are widespread. Mapping submerged macrophytes without taking into account the spectral response of water column optical features is not considered feasible without assumptions and a site-specific approach (e.g. Hunter et al., 2010). Submerged macrophytes can be on the contrary effectively mapped from EO medium resolution data when are dense enough and are present in a mixture with floating species, with no clear dominance. For these reason, the macrophyte community type scheme finally adopted as target classification legend for our mapping approach cannot fully match the macrophyte functional group categorization of Table 1. As a consequence, we grouped the six functional groups into four synthetic macrophyte community types (Fig. 2): i) helophyte, ii) emergent rhizophyte, iii) floating (i.e free-floating pleustophyte and floating-leaved rhizophyte groups merged together), and iv) submerged-floating association (i.e. the coexistence of submerged and floating macrophytes when no clear dominance in the community is identified). Even if more synthetic, this target scheme still manages to both expresses the complex mosaic of vegetation within the studied areas, in terms of influence of vegetation background, species mixture and growth forms observed.

3. Materials

3.1. In situ and reference data

In situ and reference data were collected during boat-based surveys and from ancillary digital maps, dealing with: macrophyte cover (presence/absence), dominant macrophyte species, and spectroradiometric response. For labelling each reference macrophyte stand surveyed, seasonal annual dominant community type (Fig. 2) and compositional homogeneity (major dominant species covering more than 80% of the plot) were considered. Each stand was geolocated using GPS devices with positional accuracy adequate for medium resolution data with pixel size around 30 m. Only homogeneous macrophyte stands covering an area of minimum 50 × 50 m around the sampling locations were recorded. Specific characteristics of macrophyte data collected over each site are described in the following.

For Lake Taihu, 19 sampling stations and a total of 113 macrophyte beds were surveyed: 13 for submerged, 8 for submerged-floating association, 71 for floating, and 21 for riparian helophyte community types (6 plant species, see Table 1). Data were collected during three days of intensive field campaigns covering the eastern and south-eastern parts of the lake, which are dominated by aquatic plants (July 10th–12th, 2013). Coordinates for each sample were acquired using a smartphone-integrated positioning system (GPS plus mobile network, Sony Ericsson Xperia mini pro), with planimetric accuracy around 10–20 m.

For Kis-Balaton wetland, 9 sampling stations and a total of 25 macrophyte beds were surveyed: 4 for submerged, 3 for submerged-floating association, 6 for floating, and 12 for riparian helophyte community types (11 plant species, see Table 1). Data were collected in three days on July 2014 (14th, 16th, and 18th), especially focusing on helophyte (*P. australis* and *T. angustifolia*, mainly), floating (*T. natans*, *N. lutea* and *N. alba*) and submerged (*C. demersum*, *Najas marina*) species dominant in the area. Coordinates for each sample were acquired using a handheld GPS (Trimble GeoXM), with positional accuracy of 2–5 m.

For Lake Trasimeno, 21 sampling stations for macrophytes and 10 stations for helophytes were surveyed, adding up to 31 beds: 13 for submerged, 8 for submerged-floating association, and 10 for riparian helophyte community types (9 plant species, see Table 1). Data were collected between May and September 2008, over a total of six days of field campaigns (Bresciani, Stroppiana, Fila, Montagna, & Giardino, 2009). Coordinates for each sample were acquired using a handheld GPS (Garmin eTrex H), with positional accuracy of 5–10 m.

For Mantua Lakes system, 14 sampling stations and a total of 51 macrophyte beds were surveyed: 3 for submerged, 5 for submerged-floating association, 7 for floating, 11 for emergent rhizophyte, and 25 for riparian helophyte community types (11 plant species, see Table 1). Data were collected in three dates along the growing season of 2014 (June 26th, July 25th, September 23rd). Coordinates for each sample were acquired using a handheld GPS (Trimble GeoXM), with positional accuracy of 2–5 m. For the validation of ALOS AVNIR-2 derived mapping products over the year 2010, we used the official vegetation cover map covering the whole lakes system (Rigoni & Giovagnoli, 2010), elaborated for the Mincio Regional Park authority starting from 2009 to 2010 surveys carried out according to the phytosociological approach used by Tomaselli et al. (2000).

For Lake Varese, original reference data (44 transects) were collected during traditional transect survey carried out along the lake shore in July–August 2008, from 1-m depth interval down to the maximum colonization depth, and covered all the main macrophyte types: the riparian emergent beds of *P. australis*, and the littoral stands of *C. demersum*, *N. alba*, and *T. natans* (Azzella et al., 2014b). Such data were used for assessing the macrophyte vegetation present in 2014 by checking the persistence of vegetation cover previously gathered in 2008 based on a field survey in some selected areas (4 sites, on July 23rd) and high resolution satellite images available in Google Earth (dating August 8th). From original transect observations we derived macrophyte reference community type data for a total of 13 macrophyte beds: 2 for submerged-floating association, 5 for floating, and 6 for riparian helophyte types (5 plant species, see Table 1). Coordinates for each sample were acquired using a handheld GPS, with positional accuracy of 2–4 m.

Spectroradiometric response of different macrophytes was collected *in situ* over Kis-Balaton wetland and Mantua Lakes system sites. Spectra were acquired using a portable Fieldspec FR (Analytical Spectral Devices) spectroradiometer (350–2500 nm, 1 nm resolution). The instrument was set to reflectance mode using a Spectralon diffuse white reference panel, and equipped with a lens of 5° FOV. Spectral reflectance

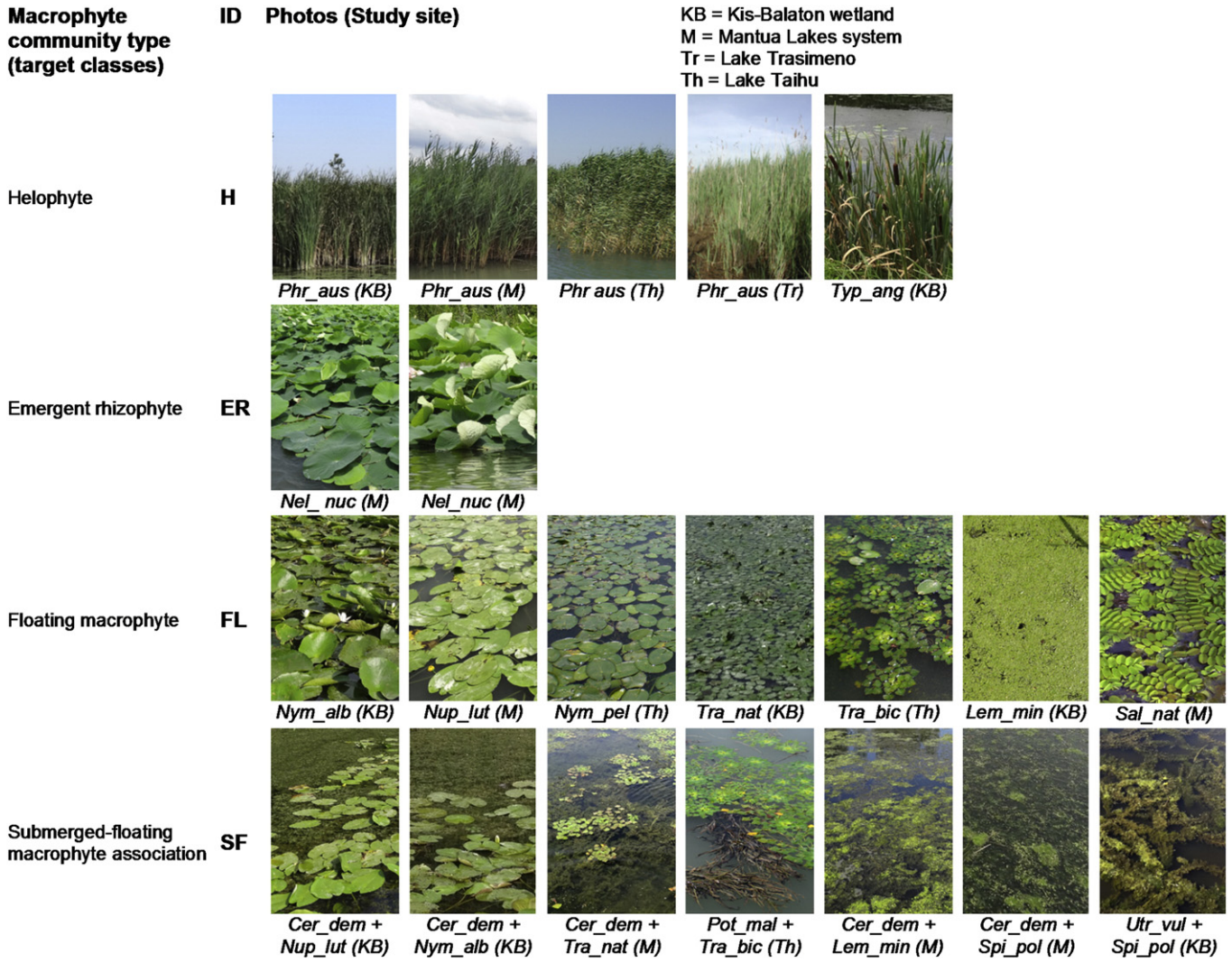

Fig. 2. Macrophyte community type scheme adopted as classification target in our work, including photos of main macrophytes types present over the test sites. The species abbreviations are as in Table 1.

response of each macrophyte sampled station was acquired from around 50 cm above plant canopy with nadir configuration. Five spectra (each being the mean value of 10 scans) per each plot were collected at maximum ±1 h of time difference of satellite (Landsat 8) overpass, and were then averaged to reproduce spectral response at OLI resolution. We acquired the averaged spectral response of homogeneous stands in terms of dominant species present, covering at least 50 × 50 m area: 6 plots on July 16th, 2014 over Kis-Balaton wetland, representing *C. demersum*, *N. alba*, and four different *T. natans* stands, and 5 plots on September 23rd, 2014 over Mantua Lakes system, representing *T. natans*, *N. lutea*, *N. nucifera*, and two *C. demersum* stands.

3.2. Satellite data

Since at medium spatial resolution the spectral discrimination capabilities currently granted by existing (e.g., Landsat 8) and near future (e.g. Sentinel-2) available EO data are quite limited for macrophyte applications, the rationale of the approach here proposed is to exploit multi-temporal information for separating and automatically mapping different macrophyte target groups and other land cover classes, commonly present in wetlands and freshwater environments (e.g. terrestrial vegetation, open water). A multi-temporal dataset of broadband satellite data, covering visible and near infrared (VNIR) spectral range between 400 and 900 nm at medium resolution (10–30 m ground pixel), was collected over the five study areas, including Landsat 7 ETM+, Landsat 8 OLI and ALOS AVNIR-2 scenes. A cloud cover threshold lower than 10% over the study sites was adopted and other data were discarded. Given this constraint, and in order to guarantee a good coverage of the growing season for 2013 in Lake Taihu and 2014 in Kis-Balaton wetland, we integrated OLI scenes available with ETM+ scenes for the two sites. Satellite dataset is composed of a total of 41 scenes: 31 scenes (ETM+ and OLI) covering four sites were used for the development of the methodology, 10 scenes (OLI and AVNIR-2) were reserved for external validation of results (Table 2).

4. Methods

4.1. Satellite data processing

Satellite data were pre-processed through radiometric calibration, followed by conversion to ground reflectance via atmospheric effect correction using ATCOR-2 code (Richter & Schläpfer, 2011). For Landsat 8 OLI data top-of-atmosphere radiance correction was applied before atmospheric correction, according to Pahlevan et al. (2014). ATCOR-2 was run with atmospheric profiles defined according to the latitude and the season of imagery, aerosol type set depending on land cover and environmental conditions of the targets and surrounding areas, and visibility derived according to the dark dense vegetation approach

Table 2
Satellite dataset overview (scenes in italic bold were used for validation only).

	Lake Taihu	Kis-Balaton wetland	Lake Trasimeno	Mantua Lakes system	Lake Varese
Landsat 7 ETM+	11 July 2013 12 August 2013	05 May 2014 21 May 2014 06 June 2014 22 June 2014 09 August 2014 12 October 2014	16 April 2008 02 May 2008 19 June 2008 05 July 2008 06 August 2008 22 August 2008 26 November 2008		
Landsat 8 OLI	14 April 2013 19 July 2013 08 November 2013 10 December 2013	27 April 2014 16 July 2014 17 August 2014 18 September 2014		07 April 2014 09 May 2014 10 June 2014 05 July 2014 28 July 2014 29 August 2014 23 September 2014 02 November 2014	***13 March 2014*** ***14 April 2014*** ***01 June 2014*** ***03 July 2014*** ***19 July 2014*** ***04 August 2014*** ***23 October 2014***
ALOS AVNIR-2				***20 April 2010*** ***21 July 2010*** ***21 October 2010***	

(Kaufman et al., 1997). For Landsat 7 ETM+ data, SLC-off gaps were filled using the approach developed by Maxwell, Schmidt, and Storey (2007).

VNIR spectral bands were isolated and retained for further processing: i.e. band 1-band5 for OLI data, band 1-band4 for ETM+ data and band 1-band 4 for AVNIR-2 data. Broadband VNIR spectra were used for deriving three distinct VIs: a generic terrestrial vegetation index, NDVI (Rouse, Haas, Schell, & Deering, 1974), and two indices recently introduced by the authors, i.e. NDAVI (Villa et al., 2013), and WAVI (Villa et al., 2014a). Both these indices have been specifically designed for capturing aquatic vegetation characteristics, through the integration of spectral response in shorter visible wavelength range. NDAVI and WAVI have been tested over a diverse dataset in terms of EO sensors and study sites in northern Italy, showing enhanced sensitivity to vegetation features and better performance in distinguishing aquatic from terrestrial vegetation, when compared to pre-existing VIs (e.g. NDVI) targeted at terrestrial vegetation (Villa et al., 2014a; Villa, Bresciani, Braga, & Bolpagni, 2014b). The equations for calculating the two VIs using spectral bands for OLI sensor are:

$$\mathrm{NDAVI} = \frac{\rho_{\mathrm{NIR}(\mathrm{OLI}_{\mathrm{band5}})} - \rho_{\mathrm{Blue}(\mathrm{OLI}_{\mathrm{band2}})}}{\rho_{\mathrm{NIR}(\mathrm{OLI}_{\mathrm{band5}})} + \rho_{\mathrm{Blue}(\mathrm{OLI}_{\mathrm{band2}})}} \quad (1)$$

$$\mathrm{WAVI} = (1+\mathrm{L}) = \frac{\rho_{\mathrm{NIR}(\mathrm{OLI}_{\mathrm{band5}})} - \rho_{\mathrm{Blue}(\mathrm{OLI}_{\mathrm{band2}})}}{\rho_{\mathrm{NIR}(\mathrm{OLI}_{\mathrm{band5}})} + \rho_{\mathrm{Blue}(\mathrm{OLI}_{\mathrm{band2}})} + \mathrm{L}} \quad (\mathrm{L} = 0.5) \quad (2)$$

An overview of macrophyte features in terms of multi-spectral and multi-temporal information is given in Fig. 3, derived from Landsat 8 OLI temporal series (April to November 2013) over Mantua Lakes system site and representing community response of homogeneous pixels (30 m) covered by different species, mainly aquatic ones. Multi-spectral response in Fig. 3a are focusing on VNIR range (OLI band1–band5), being longer wavelengths affected by the strong absorption of water which extremely diminishes the sensitivity to plant material. Multi-temporal profiles in Fig. 3b have been derived for WAVI, as best performing option in classifying terrestrial and aquatic vegetation features already tested for inland lakes in northern Italy (Villa et al., 2014b). Even if both reflectance and multi-temporal WAVI profiles highlight to a certain extent macrophyte heterogeneity in the study area, a direct comparison of graphs shows the enhanced distinction power of temporal series (Fig. 3b) for most of the species, when compared to spectral information only (Fig. 3a).

Distinct multi-temporal behaviours for different macrophyte species are evident from WAVI series for Mantua Lakes system depicted in Fig. 3b. Helophyte (*P. australis* stands) and emergent rhizophyte (*N. nucifera* stands) samples show a rapid rise (up to 0.6–0.9) in late spring, indicative of an increase in biomass and green leaves, and are generally well discriminated by the ones shown by terrestrial vegetation, represented by grassland, here dominated by *Lolium multiflorum* (Annual ryegrass) and woodland, dominated by *Salix alba* (White willow). Floating-leaved rhizophytes (*N. lutea* stands) expand their cover over the water surface later in the season and never peak at WAVI higher than 0.5, while small and dense free-floating pleustophyte (*S. natans*) stands dramatically increase in WAVI from 0.1 to over 0.5 over few weeks in late July. In addition, different maturity stages of *T. natans* show peculiar temporal-density patterns for samples collected

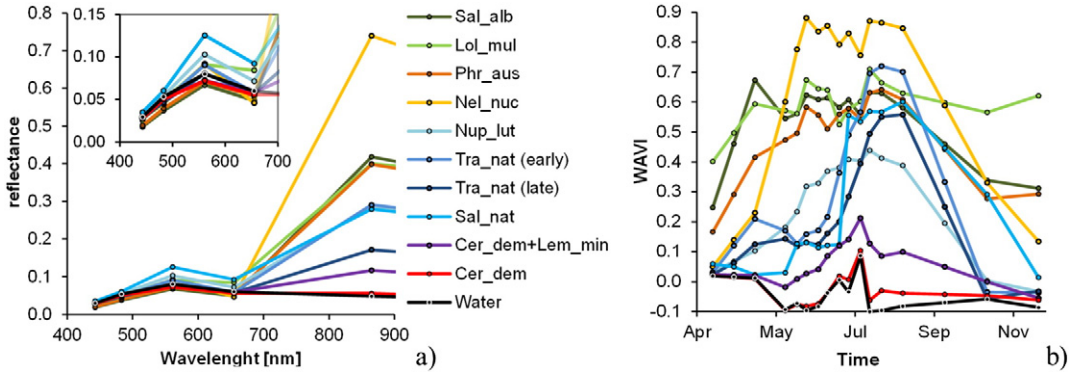

Fig. 3. Multi-spectral VNIR response in summer season conditions (August 3rd, 2013) of different terrestrial and aquatic vegetation species (a), compared to their multi-temporal WAVI profiles derived from spring–autumn 2013 (b), extracted from OLI time series over Mantua lake system site. The species abbreviations are as in Table 1, *Sal_alb* = *Salix alba*, *Lol_mul* = *Lolium multiflorum* (adapted from: Hestir et al., 2015).

in different areas over the site. At the bottom end of WAVI scores (lower than 0.2), Fig. 3b highlights stands colonized by an association of free-floating and submerged macrophytes, *C. demersum* and *L. minor*, while submerged *C. demersum* and macrophytes-free open water areas profiles are mostly overlapping.

Spectral features derived from satellite data, either surface reflectance outputs of atmospheric correction and VIs calculated for them, were assessed against *in situ* spectra of aquatic vegetation collected in Kis-Balaton wetland and Mantua Lakes system sites. *In situ* spectra were resampled for matching the VNIR Landsat 8 OLI spectral bands using band central wavelength and Full Width Half maximum values from Barsi, Lee, Kvaran, Markham, and Pedelty (2014). Resampled *in situ* spectra were compared to surface reflectance derived after radiometric and atmospheric effect correction of the OLI scenes acquired in the same days at maximum 1 h of time difference. The linear coefficient of determination (r^2), and Mean Absolute Error (MAE) between *in situ* reflectance and OLI corrected reflectance were calculated in order to assess if the accuracy of radiometric processing of satellite data was sufficient for the scope of the work.

4.2. Macrophyte community type separability

Starting from *in situ* and reference data, the information about macrophytes presence in each of the sites was summarized into georeferenced Areas of Interest (AOIs). Reference data of macrophytes were prepared starting from direct survey information collected during the same year of acquisition of the satellite dataset described in Table 2, with sampling points spatially spread over the main macrophyte-dominated areas and covering the major species present in each test site (Table 1).

As introduced in Section 2, macrophyte community types were grouped into four main target classes (Fig. 2): helophyte (H), emergent rhizophyte (ER), floating (FL), and submerged-floating macrophyte (SF). Two complementary target classes were added to the classification legend: terrestrial vegetation (TV), and open water (OW), this last including areas where submerged macrophytes are not reaching the surface of the lake and cannot therefore be effectively distinguished from water surface using broadband VNIR spectra.

Table 3 shows the cardinality and distribution of the reference AOIs, over the five sites: four used for training and internal validation and one, Lake Varese, for external validation (while Mantua Lakes system is involved for both, using different years and satellite data).

The reference dataset for the four test sites, i.e. Lake Taihu (2013), Kis-Balaton wetland (2014), Lake Trasimeno (2008), Mantua Lakes system (2014), is split into two parts: half is used for training the classifier, and the other half is used for internal validation. Since the number of plots sampled *in situ* was in general too little for most of the macrophyte community types (especially for ER and SF classes), the split was done on a per-pixel basis, with random sampling performed over the reference plot pixels stratified by target class. Descriptive statistics were extracted from the AOIs for each of the four main study sites (excluding Lake Varese, used for validation only) in the satellite dataset, under five different spectral-temporal combinations: i) VNIR(*f*S), i.e. mono-temporal VNIR band combination for full summer season conditions (July–August); ii) VIs(*f*S), i.e. mono-temporal combination of VIs (NDVI, NDAVI and WAVI) in full summer season conditions; iii) NDVI(*m-t*), i.e. multi-temporal combination of NDVI; iv) NDAVI(*m-t*), i.e. multi-temporal combination of NDAVI; and v) WAVI(*m-t*), multi-temporal combination of WAVI. NDVI(*m-t*), NDAVI(*m-t*) and WAVI(*m-t*) cover the vegetative cycle of aquatic and terrestrial vegetation in temperate to subtropical environments (Spring–Autumn: April–November). Average, variance and covariance figures for all the target cover classes AOIs were extracted, and exploited to test the separability between the different macrophyte classes (SF, FL, ER, H) and the other target classes (TV, OW). The separability assessment was run using the Jeffries–Matusita Distance (J–M_{DIST}) on a class-by-class basis. J–M_{DIST} is a commonly used as separability measure, based on Bhattacharyya distance, which assesses the similarity of two probability distributions through the amount of overlapping they show (Bhattacharyya, 1943; Swain & King, 1973). J–M_{DIST} scores range from 0 (absolutely non separable features) to 2 (complete separability). As a rule of the thumb, J–M_{DIST} scores higher than 1.9 indicate good separability, while poorly separable classes are characterized by J–M_{DIST} lower than 1.0 (Richards & Jia, 1999). J–M_{DIST} were first calculated for each pair of classes in the AOIs, and all possible pairs were then averaged into a single measure for assessing the overall separability achieved for each of the five spectral-temporal factors combinations listed above.

4.3. Macrophyte community type classification

The macrophyte community type classification approach implemented is based on a hierarchical set of cascade rules structured in a binary tree. The rule-based classification is implemented using a Classification Tree (CT) scheme. The algorithm is included in WEKA suite, as J48 routine (Witten & Frank, 2005), and is modelled on C4.5 (Quinlan, 1996). CT (J48) mainly consists of a supervised recursive partitioning algorithm, that generates a decision tree based on information gain ratio splitting criteria and supports both nominal and numeral input attributes. For the implementation of our rule-based approach, we allowed only binary splits for each node, coupled with online pruning with confidence factor of 0.25 and sub-tree raising. For minimizing over-fitting and tree size, we set the minimum number of classified instances per each final node equal to 20, less of half the size of the smallest class in the training set (54 pixels for ER, see Table 2).

This approach is both flexible and robust, and it is easily used for shaping a set of rules with optimized decision boundaries, dependent on the reference training data input to the algorithm. A variety of multi-temporal features, extracted from satellite scenes covering the macrophyte growing season (April–November), were tested as input for CT: i) WAVI(Min), i.e. the minimum value of WAVI scored over the season; ii) WAVI(Max), i.e. the maximum value of WAVI scored over the season; iii) WAVI(Stdev), i.e. the standard deviation of WAVI scores computed for the season; iv) WAVI(Skew), i.e. the asymmetry of WAVI

Table 3
Reference data of macrophyte classes used for training and validation of classification (external validation data are in italic bold), expressed in number of pixels on the satellite images (and relative areal coverage of each study site). The classes abbreviations are: SF = submerged-floating association; FL = floating; ER = emergent rhizophyte; H = helophytes; TV = terrestrial vegetation; OW = open water; np = not present.

	Training set	Site specific validation subset				*Ext. validation subset*
Class ID	Whole (4 sites)	Kis-Balaton wetland (27.2 km^2)	Mantua Lakes system (12.4 km^2)	Lake Trasimeno (125.2 km^2)	Lake Taihu (2322.1 km^2)	*Lake Varese (27.0 km^2)*
SF	102	3 (0.01%)	12 (0.08%)	51 (0.04%)	36 (0.002%)	***3 (0.01%)***
FL	241	33 (0.11%)	46 (0.33%)	np	162 (0.006%)	***213 (0.71%)***
ER	54	np	54 (0.39%)	np	np	***np***
H	400	51 (0.17%)	121 (0.88%)	136 (0.12%)	92 (0.004%)	***127 (0.42%)***
TV	814	330 (1.09%)	165 (1.20%)	95 (0.07%)	224 (0.009%)	***237 (0.79%)***
OW	921	109 (0.36%)	130 (0.95%)	376 (0.31%)	306 (0.012%)	***408 (1.36%)***

seasonal scores histogram calculated as skewness coefficient; v) WAVI(*e*Sp), i.e. the WAVI value reached in early spring conditions; vi) WAVI(*f*S), i.e. the WAVI value reached in full summer conditions; and vii) WAVI(*l*A), i.e. the WAVI value reached in late autumn conditions. Early spring, full season and late autumn conditions were depending on both the specific seasonality (including climate) of the environmental systems represented by the test sites and the timing of available satellite data (i.e. with less than 10% cloud cover, see Table 2): *e*Sp dates vary from April 7th (Mantua lakes system) to April 27th (Kis-Balaton wetland), *f*S dates vary between July 11th (Lake Taihu) and August 6th (Lake Trasimeno), and *l*A dates can range from October 12th (Kis-Balaton wetland) to November 26th (Lake Trasimeno). Four different combinations of multi-temporal features were tested as input for classification: i) Set A: including WAVI(Min), WAVI(Max), WAVI(Stdev), WAVI(Skew); ii) Set B: including WAVI(Min), WAVI(Max), WAVI(Stdev); iii) Set C: including WAVI(*e*Sp), WAVI(*f*S), WAVI(*l*S); and iv) Set D: including WAVI(*e*Sp), WAVI(Max), WAVI(*l*S). The choice of best option in terms of input dataset was made on balancing the accuracy of classification results (calculated using independent reference set reserved for validation purposes), and the complexity of CT structure (in terms of number of leaves of the rule-based tree), i.e. by looking for the maximum accuracy and selecting a sub-optimal combination only if a reduction in number of CT leaves is attained without relevant decrement in accuracy.

Furthermore, to assess the performance of the scheme implemented using CT, the results of three other commonly employed supervised classification algorithms are compared, namely: Support Vector Machines (SVM), Maximum Likelihood classification (MLC), and Multilayer Perceptron neural network (MLP). SVM implementation is based on sequential minimal optimization for training, and adopts a linear kernel (Keerthi, Shevade, Bhattacharyya, & Murthy, 2001). MLC implementation is the canonical one, based on conditional distribution of classes and Bayesian inference (Richards & Jia, 1999). MLP features one single hidden layer of neurons between the input and output layers, and non-linear activation functions (Atkinson & Tatnall, 1997).

5. Results

5.1. Satellite-derived spectral feature assessment

The performance of surface reflectance data used for input features was assessed in terms of the overall matching of reference *in situ* spectra with satellite atmospherically corrected reflectance bands, shown in Fig. 4a for Kis-Balaton macrophyte plots and in Fig. 4b for Mantua Lakes system macrophyte plots. Linear regression scored a coefficient of determination $r^2 = 0.975$ for the whole OLI surface reflectance (i.e. adding up band 1 to 5) vs. *in situ* spectra. High precision of the matching is accompanied by a slight underestimation of surface reflectance by corrected OLI data (regression line slope = 0.906). In terms of MAE (Fig. 4c), lower scores are observed over the visible range (<0.011 for OLI bands 1 to 4), and a higher but still acceptable score (0.041) for the near-infrared range (OLI band 5). Regarding the spectral VIs derived from OLI corrected bands, a generally acceptable error was observed for NDVI and NDAVI derived from OLI data (0.062–0.065), with a reduction in MAE for WAVI (0.057). The level of error in macrophytes spectral response achieved for OLI data is considered low enough not to affect substantially the further exploitation of broadband VNIR response and VIs used for developing the mapping approach described in the following.

5.2. Macrophyte community type separability assessment

From J-M_{DIST} overall average results, calculated for the five different spectral-temporal combinations considered, some separability tendencies can be highlighted (Fig. 5). A general increment in average class separability is observed when using multi-temporal VIs, with respect to using the best single-date VNIR broadband dataset (here identified with full summer season), with a rise from 1.84 to 1.93 for Lake Taihu (worst separability), and from 1.91 to 1.99 for Lake Trasimeno and Mantua Lakes system (best separability). Overall separability of macrophytes classes is still higher when using multi-temporal VIs compared to the mono-temporal combination of peak of season indices: i.e. VIs(*f*S). The separability scores achieved using VIs(*f*S) dataset are always lower than using the whole spectral information included in VNIR domain (VNIR(*f*S)). Among the different multi-temporal VIs tested, slightly better performance is achieved using aquatic vegetation indices (NDAVI and WAVI), than NDVI: ranging from 1.89 to 1.93 for Lake Taihu (worst case), and from 1.98 to 1.99 for Lake Taihu and Mantua Lakes system (best case).

The best starting conditions in terms of overall separability for the four macrophyte community types is observed for Kis-Balaton wetland site, using 2014 reference data, with J–M_{DIST} = 1.93 for VNIR(*f*S) dataset, higher than for Lake Taihu (1.84), Mantua Lakes system (1.91) and Lake Trasimeno (1.91). Multi-temporal VIs reach higher separability, practically identical for NDVI, NDAVI and WAVI (1.97–98). Similar separability to that of Kis-Balaton wetland is observed for Mantua lake system and Lake Trasimeno, in terms of J-M_{DIST} achieved using VNIR(*f*S) dataset (1.91), coupled with an increment of separability using NDVI(*m-t*) reaching 1.98, followed by a further slight increment using aquatic VIs (NDAVI and WAVI) reaching 1.99. Lake Taihu shows worst separability conditions using VNIR(*f*S) dataset (J–M_{DIST} = 1.84), and an increment in separability again is reached with NDVI(m-t), J–M_{DIST} = 1.89, and aquatic VIs, peaking at 1.93 for WAVI(*m-t*) dataset.

In terms of macrophyte class individual separability performance, Table 4 shows J–M_{DIST} gain achieved for each target class pair over the four test sites. The increment in class separability is relevant between ER and TV especially for Lake Trasimeno (+0.66–0.67), and Mantua

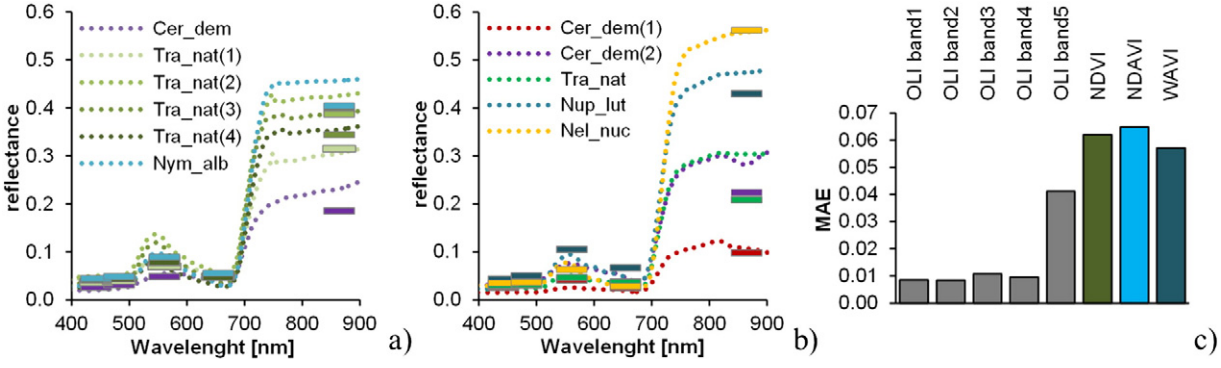

Fig. 4. Comparison of VNIR spectra collected *in situ* (dotted lines) and OLI atmospherically corrected surface reflectance bands (grey colour outlined bars): a) Kis-Balaton (July 16th, 2014) spectra, b) Mantua Lakes system (September 23rd, 2014) spectra, and c) MAE of OLI spectral bands in VNIR range (B1-B5) and spectral VIs used in the study. The species abbreviations are as in Table 1; numbers in brackets refer to different stands of the same species.

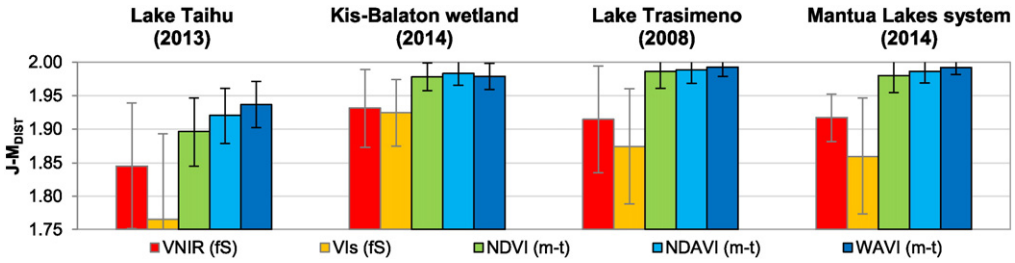

Fig. 5. Overall macrophyte community separability results (average and standard deviation) achieved using five different spectral-temporal datasets, over the four test sites.

Lakes system (+0.59–0.60) sites, when using multi-temporal VIs. For Kis-Balaton and Lake Taihu sites, the higher increment in separability is observed between SF and FL classes, with +0.35–0.37 and +0.23–0.42, respectively. This is visible for Mantua Lakes system too, even if lower in magnitude, with +0.24 gain in separability using WAVI(*m-t*). For Lake Taihu site, a slight separability enhancement is observed also between FL and H classes (+0.08–0.13). The contribution of aquatic indices to separability increment is particularly evident for H and TV class pair in Lake Taihu site (+0.22–0.30), as well as for SF and FL class pair for Lake Taihu (+0.06–0.19), and Mantua Lakes system (+0.10–0.20). Moreover, the use of multi-temporal VIs grants an increment in separability between SF and OW for Mantua Lakes system case, where starting separability is lower than for other sites ($J\text{–}M_{DIST} = 1.79$, compared to 1.95–2.00).

5.3. Macrophyte community type classification performance

Macrophyte community type classification tests were performed using the four multi-temporal features input dataset (Set A–Set D), combining all four test sites. Validation over reference dataset independent from the one used for training, calculated as Overall Accuracy (OA) and Kappa coefficient (***k***), resulted in: 90.3% OA (***k*** = 0.866) using Set A (22 total leaves in the rule based tree), 85.4% OA (***k*** = 0.797) using Set B (19 total leaves), 90.1% OA (***k*** = 0.864) using Set C (21 total leaves), and 90.2% OA (***k*** = 0.865) using Set D (20 total leaves). Taking into account both accuracy achieved and complexity of decision tree implemented, the best balance was chosen in the use of Set D as multi-temporal input for CT algorithm. The final rule-based approach was therefore implemented using tri-temporal features (Set D), including: WAVI(*e*Sp), WAVI(Max), WAVI(*l*A). The outline of macrophyte community type classification scheme adopted, showing rule thresholds and input features, is described in Fig. 6.

Fig. 6 scheme clearly highlights the clustering of macrophytes target classes mainly depending on the WAVI scores (>0.444) at the start of growing season (central node), which separates TV and H classes, less affected by water background response, from the other classes (right portion of the scheme). Left part branches feature a clear and early distinction of OW class on the basis of lower WAVI seasonal maximum scores (<0.158), as well as a sharp separation of ER class on the basis of their high WAVI maximum (>0.682). The seasonal patterns of WAVI towards autumn months (*l*A) regulate the classification of the remaining clusters into FL or SF, and OW class.

Accuracy results achieved using the CT (J48) algorithm for building our rule-based approach were compared with three other supervised classification algorithms, using the same WAVI input dataset, i.e. Set D. All tested algorithms achieved lower accuracy performance compared to the proposed approach (OA = 90.2%, ***k*** = 0.865), with best results reached with MLP (OA = 87.7%, ***k*** = 0.831), followed by SVM (OA = 85.7%, ***k*** = 0.801), and MLC (OA = 82.6%, ***k*** = 0.761).

The rule-based scheme implemented was applied to the four test sites for producing macrophyte community type maps for each water body and riparian area. Riparian areas are delimited by a buffer of 150 m from the lake shores, considering a terrain slope less than 1% (Fig. 7). From a first visual assessment, Fig. 7 maps well depict macrophyte distribution in lakes and riparian areas of European sites, with riparian belt colonized by helophytes and terrestrial vegetation and lake area showing community type dominance patterns different for each site: floating macrophytes (FL class) in Kis-Balaton wetland (Fig. 7b), submerged-floating association (SF class) in Lake Trasimeno (Fig. 7c), and a mixture of emergent rhizophytes (ER class) and floating macrophytes (FL class), with minor intrusions of submerged floating association type (SF class) in Mantua Lakes system site (Fig. 7d). For subtropical Lake Taihu, Fig. 7a maps manages to capture the large colonization of south-eastern part by floating and submerged-floating association types, but also features some misclassification of very dense floating algae as aquatic plants (FL and SF classes) in north-western bays.

Confusion matrices and class accuracies were calculated using the whole validation set and each site specific subset (see Table 3), according to Congalton (1991), and are shown in Table 5, including User's Accuracy (UA) and Producer's Accuracy (PA).

The OA retrieved for the whole dataset is 90.2% (***k*** = 0.865), and comes from the combination of site specific OA calculated for Lake Trasimeno (94.2%, ***k*** = 0.905), Kis-Balaton wetland (93.9%, ***k*** = 0.887), Mantua Lakes system (93.6%, ***k*** = 0.916), and Lake Taihu (82.8%, ***k*** = 0.762). The accuracy is very high for three of the four test sites, and lower, but still relatively good for Lake Taihu. The class specific error budget highlights the good performance of the algorithm over all the macrophyte community types (H, ER, FL) and other classes (TV, OW), with both UA and PA higher than 80%, and lower scores over SF class (UA = 65%, PA = 74%).

To test the robustness of the approach, the rule-based scheme implemented was applied to external independent validation cases, under two different configurations: i) a dataset covering an area different from the four sites utilized for developing the algorithm, Lake Varese (see rightmost column in Table 3) with multi-temporal OLI data covering 2014 growing season (Table 2), and ii) a dataset covering one of the four test sites, Mantua Lakes system, but using a different satellite sensor dataset (ALOS AVNIR-2), acquired during a season not used for implementing the approach (2010).

Macrophyte community type maps produced are shown in Fig. 8, and similarly to what happened for Fig. 7 maps are well representing the aquatic plant distribution of the two sites known from field surveys and direct knowledge of the areas. In Lake Varese, large helophyte (H class, mainly *P. australis*) beds colonize riparian and wetland areas and floating species (FL class, *T. natans* and *N. alba*) occupy the southern shores of the lake (Fig. 8a). The macrophyte map derived over Mantua Lakes system area using 2010 AVNIR-2 data (Fig. 8b) is broadly consisting with 2014 map derived from OLI data (Fig. 7d), but also shows larger areas occupied by FL class, suggesting that 2010 was meteorologically more favourable than 2014 for floating species growth (e.g. with hot summer and lower water levels, ideal conditions for *T. natans*).

Accuracy assessment for the two external validation cases gave results consistent with the ones derived for the four implementation sites: OA = 85.6% (k = 0.766) for Mantua Lakes system (AVNIR-2 2010 dataset), and OA = 94.3% (k = 0.922) for Lake Varese (OLI 2014

Table 4
Macrophytes communities separability increment compared to baseline scenario (mono-temporal VNIR(*f*S) dataset) achieved using multi-temporal VIs datasets, over the four test sites. The class abbreviations are as in Table 3, np = not present (in the site).

		Lake Taihu (2013)						Kis-Balaton wetland (2014)						Lake Trasimeno (2008)						Mantua Lakes system (2014)					
		SF	FL	ER	H	TV	OW	SF	FL	ER	H	TV	OW	SF	FL	ER	H	TV	OW	SF	FL	ER	H	TV	OW
	VNIR (*f*S)		1.40	np	1.94	2.00	1.99		1.44	np	1.97	2.00	1.95		np	np	2.00	2.00	2.00		1.63	2.00	1.98	1.99	1.79
SF	NDVI (*m-t*)		+0.23	np	+0.06	0.00	+0.01		+0.35	np	+0.02	0.00	+0.05		np	np	0.00	0.00	0.00		+0.04	0.00	+0.02	+0.01	+0.20
	NDAVI (*m-t*)		+0.27	np	+0.06	0.00	+0.01		+0.37	np	+0.03	0.00	+0.05		np	np	0.00	0.00	0.00		+0.14	0.00	+0.02	+0.01	+0.21
	WAVI (*m-t*)		+0.42	np	+0.05	0.00	+0.01		+0.35	np	+0.02	0.00	+0.05		np	np	0.00	0.00	0.00		+0.24	0.00	+0.02	+0.01	+0.21
FL	VNIR (*f*S)	1.40		np	1.80	1.99	1.99	1.44		np	1.93	2.00	2.00							1.63		2.00	2.00	2.00	1.92
	NDVI (*m-t*)	+0.23		np	+0.08	+0.01	+0.01	+0.35		np	+0.02	0.00	0.00							+0.04		0.00	0.00	0.00	+0.08
	NDAVI (*m-t*)	+0.27		np	+0.13	+0.01	+0.01	+0.37		np	+0.05	0.00	0.00							+0.14		0.00	0.00	0.00	+0.08
	WAVI (*m-t*)	+0.42		np	+0.09	+0.01	+0.01	+0.35		np	+0.04	0.00	0.00							+0.24		0.00	0.00	0.00	+0.08
ER	VNIR (*f*S)																			2.00	2.00		1.99	1.96	2.00
	NDVI (*m-t*)																			0.00	0.00		+0.01	+0.04	0.00
	NDAVI (*m-t*)																			0.00	0.00		+0.01	+0.04	0.00
	WAVI (*m-t*)																			0.00	0.00		+0.01	+0.04	0.00
H	VNIR (*f*S)	1.94	1.80	np		1.46	2.00	1.97	1.93	np		1.99	2.00	2.00	np	np		1.33	2.00	1.98	2.00	1.99		1.40	2.00
	NDVI (*m-t*)	+0.06	+0.08	np		−0.05	0.00	+0.02	+0.02	np		+0.01	0.00	0.00	np	np		+0.67	0.00	+0.02	0.00	+0.01		+0.59	0.00
	NDAVI (*m-t*)	+0.06	+0.13	np		+0.17	0.00	+0.03	+0.05	np		+0.01	0.00	0.00	np	np		+0.66	0.00	+0.02	0.00	+0.01		+0.59	0.00
	WAVI (*m-t*)	+0.05	+0.09	np		+0.25	0.00	+0.02	+0.04	np		−0.01	0.00	0.00	np	np		+0.67	0.00	+0.02	0.00	+0.01		+0.60	0.00

dataset). Confusion matrices for the two external validation sites are shown in Table 6.

6. Discussion

Results described in previous section support the feasibility of mapping four macrophyte community types (H, ER, FL, SF) distinctly from other land cover classes (TV and OW) using multi-temporal features derived from WAVI, i.e. a VI specifically introduced by the authors for aquatic vegetation.

The best performing aquatic vegetation seasonal proxy was assessed through separability analysis, with multi-temporal VIs showing higher average J-M_{DIST} (1.93–1.99), compared to mono-temporal VNIR or combined VIs (Fig. 5). Differences among test sites were observed: higher separability for Kis-Balaton wetland was due to the characteristics of TV in the area, being more different from H class here than in other sites (see Table 4), while lower separability for Lake Taihu was probably due to the local high representativeness of submerged species (see Table 1), and to the presence of dense floating algal mats forming during cyanobacteria blooms in warm season (May to September, Duan et al., 2009; Villa at al., 2015), that generates class confusion mainly between SF and FL (see Table 4). Among multi-temporal VIs tested, WAVI consistently resulted in better separability (Fig. 5), with main enhancement in class distinction capabilities concentrated on ER–TV pair for Lake Trasimeno and Mantua Lakes system, and on SF–FL pair for Kis-Balaton wetland and Lake Taihu (Table 4). Such results support the use of WAVI not only for distinguishing aquatic from terrestrial vegetation, as the authors have previously demonstrated (Villa et al., 2014a, 2014b), but also for maximizing the capabilities to distinguish and classify macrophyte community types, which would be difficult to separate using spectral information only (i.e. using VNIR(*f*S)).

Multi-temporal feature sets derived from WAVI were tested for assessing the most efficient input combination to be used for implementing a rule-based macrophyte community mapping approach, using a CT (J48) algorithm, and training samples comprising four heterogeneous test sites. Detection overall accuracy and decision tree complexity, were taken into account and best performing seasonal features were selected, composed by tri-temporal WAVI scores (Set D). The mapping approach finally implemented (Fig. 6) achieved an OA of 90.2% ($\boldsymbol{k}$ = 0.865), outperforming other supervised classification methods (MLP, SVM, and MLC). Accuracies were higher over European, temperate to Mediterranean areas (OA = 93.6–94.4%, $\boldsymbol{k}$ = 0.887–0.916), than over the subtropical Lake Taihu site (OA = 82.8%, $\boldsymbol{k}$ = 0.762), thus confirming some difficulties already observed in separability assessment over this site, all shown in Table 5 confusion matrices. Per-class accuracies (UA and PA) are consistently quite high for the temperate European sites. Mantua Lakes system 2014 map (Fig. 7d) covers all the six classes and well represent the situation depicted in reference data, with UA = 83–100% and PA = 86–100%. Very reliable results are achieved from Lake Trasimeno 2008 map (Fig. 7c) too, where four classes are distinguished reaching UA = 82–100% and PA = 85–98%, with the exception of the misclassification of a very small area (0.8 ha) as FL, a class not presents in the reference data for this site. A comparable performance is observed for the Kis-Balaton wetland map (Fig. 7b; UA = 75–100%, PA = 86–97%), with the lower scores due to some underestimation for H class, which confusion with FL is possibly connected to particular characteristics of riparian vegetation density in the Hungarian site (Zlinszky et al., 2012; Stratoulias, Balzter, Zlinszky, & Tóth, 2015); the high percentage of misclassification as open water of SF area in reference dataset is too small to be considered significant (less than 0.3 ha).

The overall relatively high rate of misclassification scored by submerged-floating association type (UA = 65%, PA = 72%, Table 5) is coming from underperformance observed for this class over Lake Taihu (UA = 22%, PA = 33%), where it is frequently confused with OW and FL classes. Lake Taihu features some peculiar characteristics

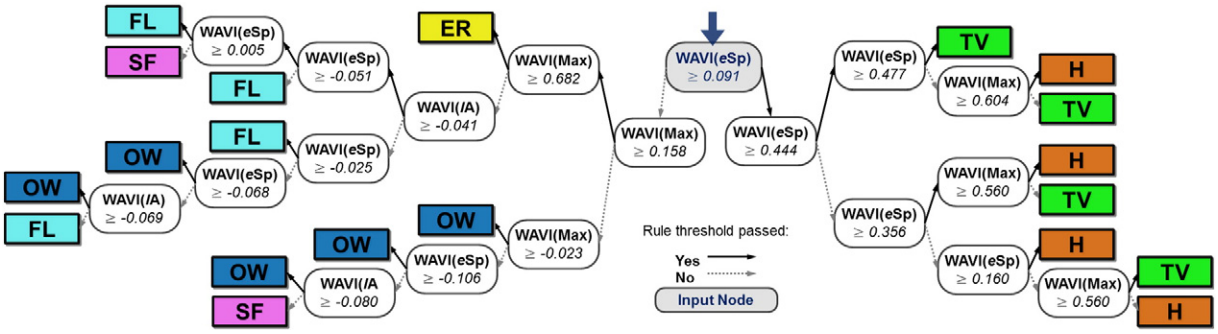

Fig. 6. Rule-based macrophyte community type classification scheme implemented, using tri-temporal features as input (Set D): WAVI(*e*Sp), WAVI(Max), WAVI(*IA*).

compared to other sites (Fig. 7a), which can explain the different accuracy patterns for this site compared to European, temperate sites: i) the floating macrophyte stands (exclusively colonized by floating-leaved *N. peltata* and *T. bicornis*) and the stands populated by submerged-floating species association typical of this site (see Table 1) can assume typical growth forms (colonizing very large areas in the south-eastern part of the lake), different form European test sites; ii) the frequent episodes of algal blooming with dense accumulation of surface scum (Duan et al., 2009; Villa et al., 2015) can strongly affect intensity and seasonality of WAVI maximum scores, thus originating misclassifications

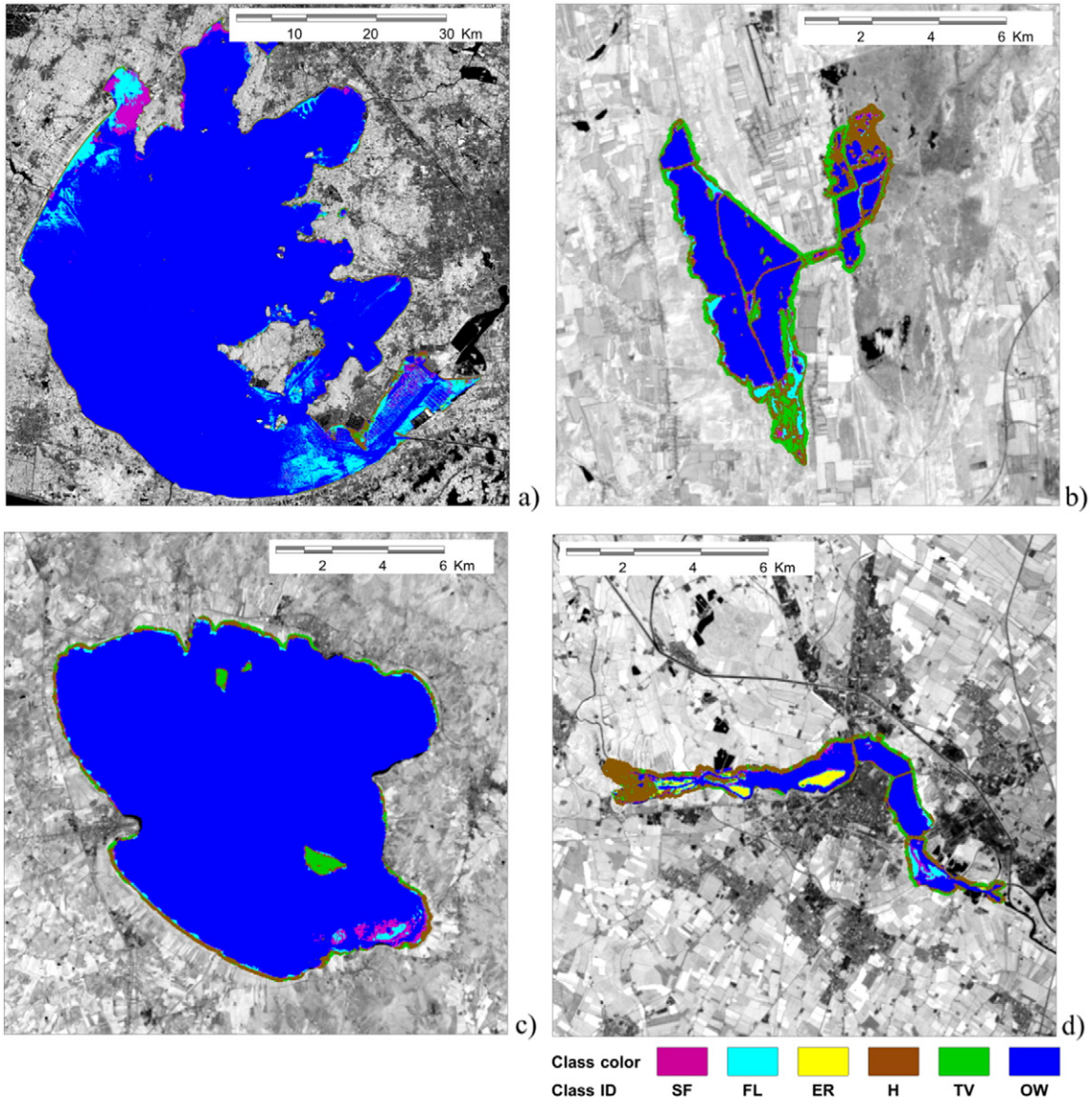

Fig. 7. Macrophyte community type maps produced using the proposed rule-based approach, for the four test sites: a) Lake Taihu (2013), b) Kis-Balaton wetland (2014), c) Lake Trasimeno (2008), d) Mantua Lakes system (2014). The class abbreviations (ID) are as in Table 3.

Table 5
Confusion matrices (figures are expressed in 30 m pixels) for the whole dataset used for independent validation over the four test sites, and for each site individually. The class abbreviations are as in Table 3; OA = Overall Accuracy; ***k*** = Kappa coefficient of agreement; UA = User's Accuracy; PA = Producer's Accuracy; np = not present (in the site); nc = not calculated.

		Whole dataset							Lake Taihu (2013)							Kis-Balaton wetland (2014)							Lake Trasimeno (2008)							Mantua Lakes system (2014)						
		Reference class							*Reference class*							*Reference class*							*Reference class*							*Reference class*						
		SF	*FL*	*ER*	*H*	*TV*	*OW*	PA	*SF*	*FL*	*ER*	*H*	*TV*	*OW*	PA	*SF*	*FL*	*ER*	*H*	*TV*	*OW*	PA	*SF*	*FL*	*ER*	*H*	*TV*	*OW*	PA	*SF*	*FL*	*ER*	*H*	*TV*	*OW*	PA
Mapped class	***SF***	66	8	1	5	0	9	**74%**	8	8	np	5	0	3	**33%**	0	0	np	0	0	6	**0%**	48	np	np	0	0	0	**100%**	10	0	1	0	0	0	**91%**
	FL	3	204	0	15	0	27	**82%**	1	131	np	14	0	15	**81%**	0	28	np	0	0	4	**87%**	0	np	np	1	0	8	**nc**	2	45	0	0	0	0	**96%**
	ER	0	0	48	0	0	0	**100%**	0	0	np	0	0	0	**nc**	0	0	np	0	0	0	**nc**	0	np	np	0	0	0	**nc**	0	0	48	0	0	0	**100%**
	H	2	7	2	320	50	0	**84%**	2	2	np	54	26	0	**64%**	0	5	np	38	1	0	**86%**	0	np	np	116	7	0	**94%**	0	0	2	112	16	0	**86%**
	TV	0	1	3	58	764	0	**92%**	0	0	np	17	198	0	**92%**	0	0	np	13	329	0	**96%**	0	np	np	19	88	0	**82%**	0	1	3	9	149	0	**92%**
	OW	31	21	0	2	0	885	**94%**	25	21	np	2	0	288	**86%**	3	0	np	0	0	99	**97%**	3	np	np	0	0	368	**99%**	0	0	0	0	0	130	**100%**
	UA	**65%**	**85%**	**89%**	**80%**	**94%**	**96%**	**OA =**	**22%**	**81%**	**nc**	**59%**	**88%**	**94%**	**OA =**	**0%**	**85%**	**nc**	**75%**	**100%**	**91%**	**OA =**	**94%**	**nc**	**nc**	**85%**	**93%**	**98%**	**OA =**	**83%**	**98%**	**89%**	**93%**	**90%**	**100%**	**OA =**
								90.2%							**82.8%**							**93.9%**							**94.2%**							**93.6%**
								k **=**							***k*** **=**							***k*** **=**							***k*** **=**							***k*** **=**
								0.865							**0.762**							**0.887**							**0.905**							**0.916**

of OW areas with FL and SF classes (northern and western bays in Fig. 7a); and finally iii) the different mixture of riparian vegetation present along the shores of Lake Taihu, with *P. australis* as dominant but not unique species (Zhao et al., 2012), as well as the different phenology of Common reed at subtropical latitude, which are probably the reason for the low UA and PA for H class (59% and 64%, respectively).

Since macrophyte stands surveyed and included into the reference dataset described in Section 3.1 were too few in number for most classes (especially for ER and SF) for allowing per-plot based splitting between training and validation subsets, the split was done on a per-pixel basis with random sampling over the reference datasets. Validation sample used for assessing the performance over the four principal test sites may therefore include some correlation with the sample used for training the classifier, and consequently bring to possible overestimation of accuracy measures illustrated in Table 5. For overcoming this issue and for giving an unbiased assessment of our mapping approach performance, its reliability and robustness were eventually validated over external, independent data (either for a different site or using different satellite data). In this context, best performance were achieved for Lake Varese map using OLI 2014 data (Table 6), with results accuracy consistent with the other European temperate sites used for implementation (see Fig. 8a): OA > 90% (***k*** > 0.90) and high per-class accuracies (UA and PA both >89%) for all classes except SF. In fact, although sparse populations of *N. marina* and *C. demersum* are present in the site (Table 1), mixture with floating species does not occur over areas large enough for a correct identification from OLI resolution. Accordingly, class errors for SF class are therefore probably biased, mostly consisting in submerged vegetation, thus falling in OW class, and no decisive statement can be made about this misclassification with the data available (SF in reference data covering less than 0.3 ha). For Mantua Lakes system map produced from 2010 AVNIR-2 data, lower overall accuracy was reached, but still quite good (OA > 85%, ***k*** > 0.75). Apart from the high errors for SF, already discussed for Lakes Taihu and Varese, underperformance here looks mainly attributable to the different spatial resolution of AVNIR-2 data (10 m), which tends to enhance class confusion where patchy vegetation mixture is present, compared to Landsat data used for other sites. FL class (UA = 55%, PA = 61%) is confused with both ER and OW, especially at the border of the larger *N. nucifera* stands and near the shores of the lake where transition from dense vegetation to open water occurs (Fig. 8b). A similar issue is evident as well in the wetland areas mainly covered by H class (UA = 74%, PA = 89%), which are confused with TV class in some cases, due to the inclusion of ruderal and arboreal species among dominant Common reed, such as *Calystegia sepium*, *Rubus* ssp., *Humulus lupulus*, *Sambucus nigra*, and *Salix cinerea* (Rigoni & Giovagnoli, 2010); these degraded patches are well visible at higher spatial resolution of AVNIR-2 data, while at Landsat resolution (i.e. over Mantua Lakes system 2014 map, Fig. 7d) they did not pop up enough for being detected as TV class. Another factor possibly affecting the mapping performance for Mantua 2010 case is that the multi-temporal dataset is composed of only three dates (Table 2), thus limiting the chances to fully exploit the seasonal maximum input feature; WAVI(Max) value is in fact fixed at the unique summer season scene (July 21st), while over other test sites the algorithm was based on selecting the peak value during the whole summer, covering 3–5 dates in July–August range.

We have to remark that the proposed approach does not allow the identification of submerged macrophyte as an independent class, being SF including submerged species only when present in association with floating ones. While submerged plants have been mapped with relative success in previous works using remote sensing in clear water small lakes (e.g. Nelson et al., 2006; Hestir et al., 2008; Hunter et al., 2010), the majority of shallow lakes in temperate areas, as in the test sites considered here, are usually turbid systems. Indeed, low transparency of water column may severely affect the capabilities of satellite data of detecting benthic vegetation (e.g. Hunter et al., 2010). Efficient mapping of submerged macrophytes as independent class in turbid

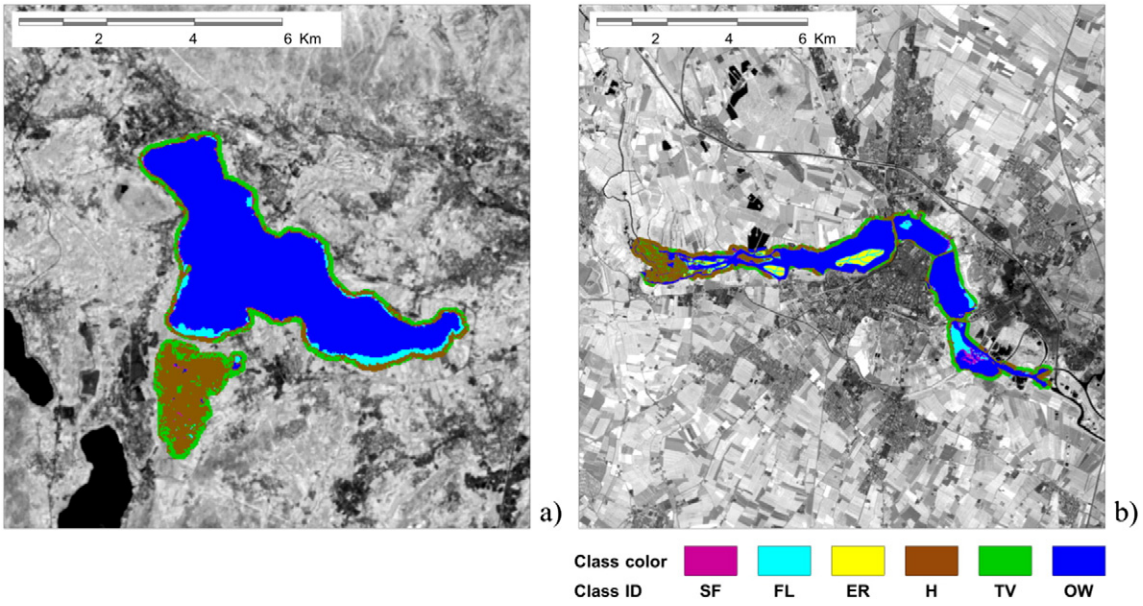

Fig. 8. Macrophyte community type maps produced using the proposed rule-based approach, over the two external validation sites: a) Lake Varese (2014, using OLI data), b) Mantua Lakes system (2010, using ALOS AVNIR-2 data). The class abbreviations (ID) are as in Table 3.

systems would therefore need further work and possibly the integration of other data sources. Nevertheless, SF class mapped with our approach can give a partial but still useful assessment of submerged plants presence and density, highlighting the areas so densely colonized by this aquatic vegetation to overcome turbidity effect and coupled with floating species usually coexisting in such communities, as *L. minor*, *S. polyrrhiza*, or *S. natans*. Even without directly mapping submerged species as an individual class, we believe that our approach has demonstrated good capabilities in capturing patterns of macrophyte community types which are environmentally important and globally widespread in temperate to subtropical areas, and this point can be the basis for further advancements in macrophyte spatial-temporal studies at regional to global scales, a crucial step for the future of aquatic vegetation remote sensing.

Compared to results described in scientific literature aiming at classifying macrophytes, our approach performance (OA = 90.2%, $\boldsymbol{k}$ = 0.865, over four macrophyte classes) is generally in line with the recent works of Wang et al. (2012) and Zhao et al. (2012), which achieved OA between 90 and 95% ($\boldsymbol{k}$ ~ 0.86–0.92) over four and three classes respectively, and better than what achieved by the works of Hestir et al. (2008) and Hunter et al. (2010) over two and four classes, respectively (OA ~ 78–80%, $\boldsymbol{k}$ ~ 0.61–0.72). Comparison is more difficult for per-class performance, being each work in the literature based on slightly different nomenclatures and schemes. Class accuracy of emergent vegetation, derived from the fusion of H and ER class with our approach, scored an average between UA and PA between 82 and 95%, slightly lower but still not distant from accuracy reached for comparable classes in other works (Hunter et al., 2010; Wang et al., 2012; Zhao et al., 2012), in the range 91–96%. Similar figures are shown over floating macrophytes, with averaged UA and PA of FL class mapped by our method (~83–84%) still lower than results of better performing approaches (~90–95%: Wang et al., 2012; Zhao et al., 2012), and comparable with results published by Hestir et al. (2008) and Hunter et al. (2010), ranging from 63 to 90%, especially if we consider results only for European temperate sites (~86–97%). As already remarked, submerged macrophytes are not treated as independent class in our approach and therefore the comparison of our output SF class (average accuracy ~70%) with submerged macrophyte mapping performance in other works cannot be done rigorously. Our approach goes beyond the results published in papers cited, dealing with site-specific (Hestir et al., 2008; Hunter et al., 2010; Wang et al., 2012; Zhao et al., 2012) or with multi-site studies (Nelson et al., 2006), because it has proven effective over a set of heterogeneous sites even on external, independent data. Another advantage of our method, not explored in previous literature, is the capability of distinguishing two types of above-water canopy-forming aquatic vegetation, as helophytes and emergent rhizophytes.

The joint use of macrophyte community type maps and multi-temporal WAVI data, highly sensitive to vegetation fractional cover and LAI (Villa et al., 2014a), can provide spatial-temporal information on aquatic vegetation seasonality characteristics. Fig. 9 shows how temporal profiles of WAVI extracted from OLI for 2014 growing season (April–October) and stratified by community type mapped in Mantua

Table 6
Confusion matrices (figures are expressed in pixels) for the external validation sites. Pixel size varies: 30 m for Lake Varese (2014) site, 10 m for Mantua Lakes system (2010) site. The class abbreviations are as in Table 3; UA = User's Accuracy; PA = Producer's Accuracy; np = not present (in the site); nc = not calculated.

		Lake Varese (2014)							Mantua Lakes system (2010)						
		Reference class							*Reference class*						
		SF	*FL*	*ER*	*H*	*TV*	*OW*	PA	*SF*	*FL*	*ER*	*H*	*TV*	*OW*	PA
Mapped class	***SF***	0	0	np	0	0	34	**0%**	117	1528	190	90	21	143	**6%**
	FL	3	211	np	6	0	0	**96%**	11	3797	1995	206	25	161	**61%**
	ER	0	2	np	3	2	0	**nc**	0	4	3844	24	4	15	**99%**
	H	0	0	np	113	1	0	**99%**	0	419	141	13,406	3011	4	**79%**
	TV	0	0	np	5	234	0	**98%**	0	20	76	2241	3103	0	**57%**
	OW	0	0	np	0	0	374	**100%**	255	1078	172	67	37	46,960	**97%**
	UA	**0%**	**99%**	**nc**	**89%**	**99%**	**92%**	**OA = 94.3% k = 0.922**	**31%**	**55%**	**60%**	**84%**	**50%**	**99%**	**OA = 85.6% k = 0.766**

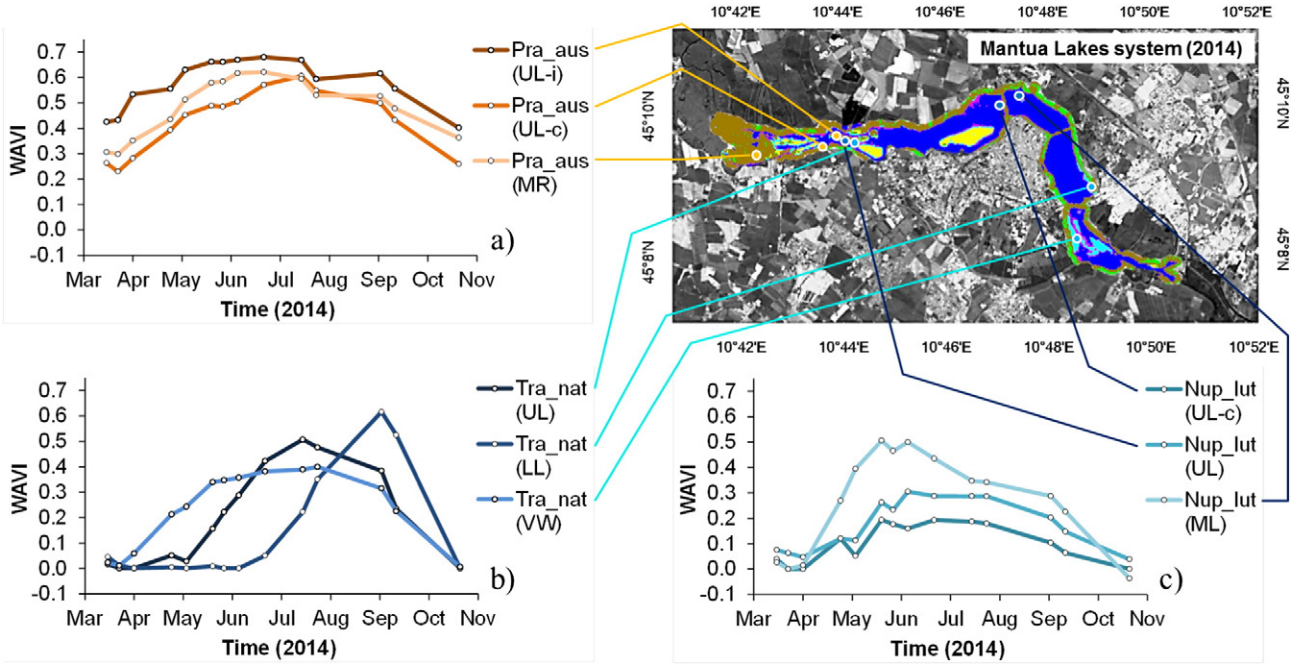

Fig. 9. Multi-temporal WAVI profiles extracted from 2014 OLI series over Mantua Lakes system macrophytes stands mapped (Fig. 7d) as helophyte (*P. australis*, panel a) and floating macrophyte (*T. natans*, panel b; *N. lutea*, panel c) community types. The species abbreviations are as in Table 1; MR = Mincio River; UL = Upper Lake; ML = Middle Lake; LL = Lower lake; VW = Vallazza wetland; c = coastal area; i = island area.

Lakes system site (as in Fig. 7d) could be exploited to assess specific phenological cycles of different community types and species for a specific year (2014). Helophyte stands in the area, dominated by *P. australis*, show a gradual increment in vegetation vigour up to June–July, more rapid and intense (higher WAVI plateau) in compact stands growing on islands within Upper Lake than along the lake coastal area (Fig. 9a). Floating macrophyte stands show a diverse seasonality, depending on the species and the location within the lakes system: *T. natans* stands growing in lower stream Vallazza wetland emerge early in May, while in Upper Lake the peak of season is reached in July, and in Lower Lake maximum density for this floating plant stands is reached only in September (Fig. 9b); *N. lutea* instead exhibits more homogeneous seasonality, with peak of season (and WAVI) reached around June, even if at different WAVI scores indicating a gradient of maximum density for this species between Middle Lake and Upper Lake stands, especially the ones growing along the coastal area (Fig. 9c).

Given the good reliability demonstrated over the environmental heterogeneous dataset, and with the upcoming generation of multi-spectral platforms (including Landsat 8 OLI), with Sentinel-2 MSI expected to be in fully operational two satellite constellation by 2017, a further advancement of testing and application of the approach implemented could be soon possible over larger areas and mapping scales. Moreover, WAVI can be calculated from broad spectral bands available for a range of EO satellites, and the approach could be easily adapted for being applied to local scale mapping of macrophytes communities using high spatial resolution sensors (e.g. Quickbird, RapidEye, WorldView-2 and -3).

The ability to obtain a clear separation between macrophyte community types allows a clear representation of the complexity of aquatic environments. Our approach goes beyond the formalization of vegetation maps, and coupled with water quality/colour monitoring can contribute to a satellite-based suite aimed at assessing the dynamics processes of inland water ecosystems under multiple temporal and spatial scales. As stressed by many previous studies, the mutual relationships and the shifts in dominance between aquatic primary producers (macrophytes and phytoplankton) reflect the environment quality or the existence of worsening trends (e.g. Kosten et al., 2011; Bolpagni et al., 2014). The recent review work of de Tezanos Pinto and O'Farrell (2014) highlighted that macrophyte role in aquatic systems regime shifts still needs extensive investigation, and we believe that the macrophyte mapping approach proposed, even if not providing direct information on submerged species as independent class, can effectively improve the knowledge on this topic by greatly expanding the amount of evidence available.

7. Conclusions

A rule-based mapping scheme for classifying four macrophyte community types was implemented over four environmentally heterogeneous inland shallow systems. Best performing input features were derived from multi-temporal WAVI, a specific aquatic vegetation index. The mapping approach was validated on two external independent cases, with accuracy results consistently in line with recent and current literature of site-specific macrophyte classification approaches, especially over European temperate areas.

Our findings demonstrate that mapping macrophyte community types of over different systems is feasible using medium-resolution, operational satellite data in a simple and straightforward way. This constitute a step forward for macrophyte mapping going beyond the local scale, and can be used for supporting regional to continental monitoring of spatial and temporal dynamics of primary produces in freshwater ecosystems. A broad scale assessment of macrophyte cover and dynamics can extend and improve the knowledge of aquatic regime shifts mechanisms.

Acknowledgements

The research leading to these results has received funding from the European Community's Seventh Framework Programme [FP7/2007–2013] under grant agreement no. 606865 (INFORM). Landsat 7 ETM + and Landsat 8 OLI data were collected from USGS Earthexplorer portal (http://earthexplorer.usgs.gov/); AVNIR-2 data were collected from ESA Eolisa portal under AO-553 MELINOS project. We thank the two anonymous reviewers whose comments helped improve and clarify

this manuscript. For having assisted in macrophyte field data collection the authors thank: Hongtao Duan and Juhua Luo, of the Nanjing Institute of Geography & Limnology, Chinese Academy of Sciences (Nanjing, China)—Lake Taihu 2013 campaigns; Matyas Presing and Victor Toth, of the Balaton Limnological Research Institute of the Hungarian Academy of Sciences (Tihany, Hungary)—Kis-Balaton wetland 2014 campaign, and Mauro Musanti, of the Institute for Electromagnetic Sensing of the Environment, National Research Council of Italy (Milan, Italy)—Lake Trasimeno 2008 campaigns.

Appendix A. Supplementary data

Supplementary data to this article can be found online at http://dx.doi.org/10.1016/j.rse.2015.10.020.

References

Abril, G., Martinez, J. M., Artigas, L. F., Moreira-Turcq, P., Benedetti, M. F., Vidal, L., ... Roland, F. (2013). *Amazon River carbon dioxide outgassing fuelled by wetlands*. Nature.

Adam, E., Mutanga, O., & Rugege, D. (2010). Multispectral and hyperspectral remote sensing for identification and mapping of wetland vegetation: A review. *Wetlands Ecology and Management*, *18*(3), 281–296.

Albright, T. P., & Ode, D. J. (2011). Monitoring the dynamics of an invasive emergent macrophyte community using operational remote sensing data. *Hydrobiologia*, *661*, 469–474.

Artigas, F. J., & Yang, J. S. (2005). Hyperspectral remote sensing of marsh species and plant vigour gradient in the New Jersey meadowlands. *International Journal of Remote Sensing*, *26*(23), 5209–5220.

Atkinson, P. M., & Tatnall, A. R. L. (1997). Introduction neural networks in remote sensing. *International Journal of Remote Sensing*, *18*(4), 699–709.

Azzella, M. M., Bolpagni, R., & Oggioni, A. (2014b). A preliminary evaluation of lake morphometric traits influence on the maximum growing depth of macrophytes. *Journal of Limnology*, *73*(2), 400–406.

Azzella, M. M., Rosati, L., Iberite, M., Bolpagni, R., & Blasi, C. (2014a). Changes in aquatic plants in the Italian volcanic-lake system detected using current data and historical records. *Aquatic Botany*, *112*, 41–47.

Barsi, J. A., Lee, K., Kvaran, G., Markham, B. L., & Pedelty, J. A. (2014). The spectral response of the Landsat-8 operational land imager. *Remote Sensing*, *6*(10), 10232–10251.

Ben-Dor, E., Schlapfer, D., Plaza, A. J., & Malthus, T. (2013). Hyperspectral Remote Sensing. In M. Wendisch, & J. -L. Brenguier (Eds.), *Airborne Measurements for Environmental Research: Methods and Instruments. 2013*, . Wiley-VCH verlag GmbH & Co. KGaA.

Bhattacharyya, A. (1943). (1943). On a measure of divergence between two statistical populations defined by their probability distributions. *Bulletin of the Calcutta Mathematical Society*, *35*, 99–109 (MR 0010358).

Birk, S., & Ecke, F. (2014). The potential of remote sensing in ecological status assessment of coloured lakes using aquatic plants. *Ecological Indicators*, *46*, 398–406.

Bolpagni, R., Bresciani, M., Laini, A., Pinardi, M., Matta, E., Ampe, E. M., ... Bartoli, M. (2014). Remote sensing of phytoplankton–macrophyte coexistence in shallow hypereutrophic fluvial lakes. *Hydrobiologia*, *737*(1), 67–76.

Bolpagni, R., Pierobon, E., Bartoli, M., Nizzoli, D., Tomaselli, M., & Viaroli, P. (2007). Methane and carbon dioxide water atmosphere daily exchanges in an oxbow lake with a *Trapa natans* stand. *Aquatic Botany*, *87*, 43–48.

Bresciani, M., Bolpagni, R., Braga, F., Oggioni, A., & Giardino, C. (2012). Retrospective assessment of macrophytic communities in southern Lake Garda (Italy) from in situ and MIVIS (Multispectral Infrared and Visible Imaging Spectrometer) data. *Journal of Limnology*, *71*, 180–190.

Bresciani, M., Stroppiana, D., Fila, G., Montagna, M., & Giardino, C. (2009). Monitoring reed vegetation in environmentally sensitive areas in Italy. *Italian Journal of Remote Sensing.*, *41*(2), 125–137.

Brown, M. E., De Beurs, K. M., & Marshall, M. (2012). Global phenological response to climate change in crop areas using satellite remote sensing of vegetation, humidity and temperature over 26 years. *Remote Sensing of Environment*, *126*, 174–183.

Caloz, R., & Collet, C. (1997). Geographic information systems (GIS) and remote sensing in aquatic botany: methodological aspects. *Aquatic Botany*, *58*(3), 209–228.

Carlson, T. N., & Ripley, D. A. (1997). On the relation between NDVI, fractional vegetation cover, and leaf area index. *Remote Sensing of Environment*, *62*(3), 241–252.

Carmichael, M. J., Bernhardt, S. E., Brauer, S. L., & Smith, W. K. (2014). The role of vegetation in methane flux to the atmosphere: Should vegetation be included as a distinct category in the global methane budget? *Biogeochemistry*, *119*(1–3), 1–24.

Chambers, P. A., Lacoul, P., Murphy, K. J., & Thomaz, S. M. (2008). Global diversity of aquatic macrophytes in freshwater. *Hydrobiologia*, *595*(1), 9–26.

Congalton, R. G. (1991). A review of assessing the accuracy of classifications of remotely sensed data. *Remote Sensing of Environment*, *37*(1), 35–46.

Cook, C. D. K. (1990). *Aquatic plant book*. The Hague: SPB Academic Publishing, 228.

Crow, G. E. (1993). Species diversity in aquatic angiosperms: Latitudinal patterns. *Aquatic Botany*, *44*(2), 229–258.

Dinka, M., Ágoston-Szabó, E., Urbanc-Berčič, O., Germ, M., Šraj-Kržič, N., & Gaberščik, A. (2008). *Reed stand conditions at selected wetlands in Slovenia and Hungary*. Netherlands: Springer, 1–12.

Dronova, I., Gong, P., Clinton, N. E., Wang, L., Fu, W., Qi, S., & Liu, Y. (2012). Landscape analysis of wetland plant functional types: The effects of image segmentation scale, vegetation classes and classification methods. *Remote Sensing of Environment*, *127*, 357–369.

Duan, H., Ma, R., Xu, X., Kong, F., Zhang, S., Kong, W., ... Shang, L. (2009). Two-decade reconstruction of algal blooms in China's Lake Taihu. *Environmental Science & Technology*, *43*(10), 3522–3528.

Duarte, C. M., Losada, I. J., Hendriks, I. E., Mazarrasa, I., & Marbà, N. (2013). The role of coastal plant communities for climate change mitigation and adaptation. *Nature Climate Change*, *3*(11), 961–968.

Duarte, C. M., Middelburg, J. J., & Caraco, N. (2005). Major role of marine vegetation on the oceanic carbon cycle. *Biogeosciences*, *2*(1), 1–8.

Dudgeon, D., Arthington, A. H., Gessner, M. O., Kawabata, Z. I., Knowler, D. J., Lévêque, C., ... Sullivan, C. A. (2006). Freshwater biodiversity: Importance, threats, status and conservation challenges. *Biological Reviews*, *81*(2), 163–182.

Farmer, A. M., & Adams, M. S. (1989). A consideration of the problems of scale in the study of the ecology of aquatic macrophytes. *Aquatic Botany*, *33*(3), 177–189.

Fensholt, R., & Proud, S. R. (2012). Evaluation of Earth Observation based global long term vegetation trends—Comparing GIMMS and MODIS global NDVI time series. *Remote Sensing of Environment*, *119*, 131–147.

Finlayson, C. M., Davis, J. A., Gell, P. A., Kingsford, R. T., & Parton, K. A. (2013). The status of wetlands and the predicted effects of global climate change: The situation in Australia. *Aquatic Sciences*, *75*(1), 73–93.

Giardino, C., Bartoli, M., Candiani, G., Pellegrini, L., & Bresciani, M. (2007). Recent changes in macrophyte colonisation patterns: An imaging spectrometry-based evaluation of southern Lake Garda (northern Italy). *Journal of Applied Remote Sensing*, *1*(1) (011509-011509).

Giardino, C., Bresciani, M., Valentini, E., Gasperini, L., Bolpagni, R., & Brando, V. E. (2015). Airborne hyperspectral data to assess suspended particulate matter and aquatic vegetation in a shallow and turbid lake. *Remote Sensing of Environment*, *157*, 48–57.

Gilmore, M. S., Wilson, E. H., Barrett, N., Civco, D. L., Prisloe, S., Hurd, J. D., & Chadwick, C. (2008). Integrating multi-temporal spectral and structural information to map wetland vegetation in a lower Connecticut River tidal marsh. *Remote Sensing of Environment*, *112*(11), 4048–4060.

Gray, J., & Song, C. (2012). Mapping leaf area index using spatial, spectral, and temporal information from multiple sensors. *Remote Sensing of Environment*, *119*, 173–183.

Hestir, E. L., Brando, V., Bresciani, M., Giardino, C., Matta, E., Villa, P., & Dekker, A. (2015). Measuring freshwater aquatic ecosystems: The need for a hyperspectral global mapping satellite mission. *Remote Sensing of Environment*, *167*, 181–195.

Hestir, E. L., Khanna, S., Andrew, M. E., Santos, M. J., Viers, J. H., Greenberg, J. A., ... Ustin, S. L. (2008). Identification of invasive vegetation using hyperspectral remote sensing in the California Delta ecosystem. *Remote Sensing of Environment*, *112*(11), 4034–4047.

Hicks, A. L., & Frost, P. C. (2011). Shifts in aquatic macrophyte abundance and community composition in cottage developed lakes of the Canadian Shield. *Aquatic Botany*, *94*(1), 9–16.

Hmimina, G., Dufrêne, E., Pontailler, J. Y., Delpierre, N., Aubinet, M., Caquet, B., ... Soudani, K. (2013). Evaluation of the potential of MODIS satellite data to predict vegetation phenology in different biomes: An investigation using ground-based NDVI measurements. *Remote Sensing of Environment*, *132*, 145–158.

Hu, C. (2009). A novel ocean color index to detect floating algae in the global oceans. *Remote Sensing of Environment*, *113*(10), 2118–2129.

Hu, C., Li, D., Chen, C., Ge, J., Muller-Karger, F. E., Liu, J., ... He, M. X. (2010). On the recurrent Ulva prolifera blooms in the Yellow Sea and East China Sea. *Journal of Geophysical Research*, *115*(C5).

Huete, A., Justice, C., & Liu, H. (1994). Development of vegetation and soil indices for MODIS-EOS. *Remote Sensing of Environment*, *49*(3), 224–234.

Hunter, P. D., Gilvear, D. J., Tyler, A. N., Willby, N. J., & Kelly, A. (2010). Mapping macrophytic vegetation in shallow lakes using the Compact Airborne Spectrographic Imager (CASI). *Aquatic Conservation: Marine and Freshwater Ecosystems*, *20*, 717–727.

Jacobs, A. E., & Harrison, J. A. (2014). Effects of floating vegetation on denitrification, nitrogen retention, and greenhouse gas production in wetland microcosms. *Biogeochemistry*, *119*(1–3), 51–66.

Jeppensen, E., Jensen, J. P., Søndergaard, M., Lauridsen, T., Pedersen, L. J., & Jensen, L. (1997). Top-down control in freshwater lakes: The role of nutrient state, submerged macrophytes and water depth. *Hydrobiologia*, *342*(343), 151–164.

Jeppesen, E., Kronvang, B., Olesen, J. E., Audet, J., Søndergaard, M., Hoffmann, C. C., ... Özkan, K. (2010). Climate change effects on nitrogen loading from cultivated catchments in Europe: Implications for nitrogen retention, ecological state of lakes and adaptation. *Hydrobiologia*, *663*, 1–21.

Jordan, S. J., Stoffer, J., & Nestlerode, J. A. (2011). Wetlands as sinks for reactive nitrogen at continental and global scales: A meta-analysis. *Ecosystems*, *14*(1), 144–155. http://dx.doi.org/10.1007/s10021-010-9400-z.

Kaufman, Y. J., Tanré, D., Remer, L. A., Vermote, E. F., Chu, A., & Holben, B. N. (1997). Operational remote sensing of tropospheric aerosol over land from EOS moderate resolution imaging spectroradiometer. *Journal of Geophysical Research: Atmospheres*, *102*(D14), 17051–17067.

Keerthi, S. S., Shevade, S. K., Bhattacharyya, C., & Murthy, K. R. K. (2001). Improvements to Platt's SMO Algorithm for SVM classifier design. *Neural Computation*, *13*(3), 637–649.

Klemas, V. (2013). Remote sensing of emergent and submerged wetlands: An overview. *International Journal of Remote Sensing*, *34*(18), 6286–6320.

Kosten, S., Jeppesen, E., Huszar, V. L. M., Mazzeo, N., Nes, E. H. V., Peeters, E. T. H. M., & Scheffer, M. (2011). Ambiguous climate impacts on competition between submerged macrophytes and phytoplankton in shallow lakes. *Freshwater Biology*, *56*, 1540–1553.

Lacoul, P., & Freedman, B. (2006). Environmental influences on aquatic plants in freshwater ecosystems. *Environmental Reviews*, *14*(2), 89–136.

Liira, J., Feldmann, T., Mäemets, H., & Peterson, U. (2010). Two decades of macrophyte expansion on the shores of a large shallow northern temperate lake—A retrospective series of satellite images. *Aquatic Botany*, *93*(4), 207–215.

Liu, Y. Y., Dijk, A. I., McCabe, M. F., Evans, J. P., & Jeu, R. A. (2013). Global vegetation biomass change (1988–2008) and attribution to environmental and human drivers. *Global Ecology and Biogeography*, *22*(6), 692–705.

Liu, W. L., Hu, W. P., Chen, Y. G., Gu, X. H., Hu, Z. X., Chen, Y. W., & Ji, J. (2007). Temporal and spatial variation of aquatic macrophytes in West. *Taihu Lake Acta Ecologica Sinica*, *27*(1), 159–170.

Lunetta, R. S., Knight, J. F., Ediriwickrema, J., Lyon, J. G., & Worthy, L. D. (2006). Land-cover change detection using multi-temporal MODIS NDVI data. *Remote Sensing of Environment*, *105*(2), 142–154.

Maxwell, S. K., Schmidt, G. L., & Storey, J. C. (2007). A multi-scale segmentation approach to filling gaps in Landsat ETM+ SLC-off images. *International Journal of Remote Sensing*, *28*(23), 5339–5356.

Mckee, D., Hatton, K., Eaton, J. W., Atkinson, D., Atherton, A., Harvey, I., & Moss, B. (2002). Effects of simulated climate warming on macrophytes in freshwater microcosm communities. *Aquatic Botany*, *74*, 71–83.

Mcleod, E., Chmura, G. L., Bouillon, S., Salm, R., Björk, M., Duarte, C. M., ... Silliman, B. R. (2011). A blueprint for blue carbon: toward an improved understanding of the role of vegetated coastal habitats in sequestering CO2. *Frontiers in Ecology and the Environment*, *9*(10), 552–560.

Millennium Ecosystem Assessment (2005). *Ecosystems and human well-being: Wetlands and water*. Washington DC.: World Resources Institute1-56973-597-2, 68.

Munyati, C. (2000). Wetland change detection on the Kafue flats, Zambia, by classification of a multitemporal remote sensing image dataset. *International Journal of Remote Sensing*, *21*(9), 1787–1806.

Nelson, S. A., Cheruvelil, K. S., & Soranno, P. A. (2006). Satellite remote sensing of freshwater macrophytes and the influence of water clarity. *Aquatic Botany*, *85*(4), 289–298.

Ning, J., Pan, H., Chen, F., & Liu, Z. (2013). Phosphorus release of metazoan zooplankton in two bays with different trophic status in Lake Taihu (China). *Knowledge and Management of Aquatic Ecosystems*, *409*, 02.

Pahlevan, N., Lee, Z., Wei, J., Schaaf, C. B., Schott, J. R., & Berk, A. (2014). On-orbit radiometric characterization of OLI (Landsat-8) for applications in aquatic remote sensing. *Remote Sensing of Environment*, *154*, 272–284.

Penuelas, J., Gamon, J. A., Griffin, K. L., & Field, C. B. (1993). Assessing community type, plant biomass, pigment composition, and photosynthetic efficiency of aquatic vegetation from spectral reflectance. *Remote Sensing of Environment*, *46*(2), 110–118.

Pettorelli, N., Vik, J. O., Mysterud, A., Gaillard, J. M., Tucker, C. J., & Stenseth, N. C. (2005). Using the satellite-derived NDVI to assess ecological responses to environmental change. *Trends in Ecology & Evolution*, *20*(9), 503–510.

Pinardi, M., Bartoli, M., Longhi, D., & Viaroli, P. (2011). Net autotrophy in a fluvial lake: The relative role of phytoplankton and floating-leaved macrophytes. *Aquatic Sciences*, *73*(3), 389–403.

Poff, N. L., Brinson, M. M., & Day, J. W. (2002). *Aquatic ecosystems and global climate change. 44*, Arlington, VA: Pew Center on Global Climate Change.

Quinlan, J. R. (1996). Improved use of continuous attributes in C4.5. *Journal of Artificial Intelligence Research*, *4*, 77–90.

Ribaudo, C., Bartoli, M., Racchetti, E., Longhi, D., & Viaroli, P. (2011). Seasonal fluxes of O_2, DIC and CH_4 in sediments with *Vallisneria spiralis*: indications for radial oxygen loss. *Aquatic Botany*, *94*, 134–142.

Richards, J. A., & Jia, X. (1999). *Remote sensing digital image analysis: An introduction* (3rd ed.). Berlin, Germany: Springer-Verlag, 240–245.

Richter, R., & Schläpfer, D. (2011). *Atmospheric/topographic correction for satellite imagery, DLR report DLR-IB 565-02/11, Wessling (D), 202.*

Rigoni, P., & Giovagnoli, G. (2010). *Carta della Vegetazione (Tav. 5), in: Piano di gestione del SIC IT20B0017 "Ansa e Valli del Mincio" e della ZPS IT20B0009 "Valli del Mincio".* (url: http://www.parcodelmincio.it/pdf/piani2010/piano valli/T5_vallimincio_vegetazione.pdf (last accessed on 11 August 2015)).

Rouse J.W., Haas R.H. Jr, Schell J.A., & Deering D.W. (1974). Monitoring vegetation systems in the Great Plains with ERTS, NASA SP-351—Washington D.C., pp. 309–317.

Schaepman, M. E., Ustin, S. L., Plaza, A. J., Painter, T. H., Verrelst, J., & Liang, S. (2009). Earth system science related imaging spectroscopy—An assessment. *Remote Sensing of Environment*, *113*, S123–S137.

Schmieder, K. (2004). European lake shores in danger—Concepts for a sustainable development. *Limnologica*, *34*, 3–14.

Schriver, P., Bogestrand, J., Jeppensen, E., & Sondergaard, M. (1995). Impact of submerge macrophytes on fish-zooplankton interactions: Large-scale enclose experiments in a shallow eutrophic lake. *Freshwater Biology*, *33*, 255–270.

Sculthorpe, C. D. (1967). *The biology of aquatic vascular plants.* London: Edward Arnold, 610.

Shuchman, R. A., Sayers, M. J., & Brooks, C. N. (2013). Mapping and monitoring the extent of submerged aquatic vegetation in the Laurentian Great Lakes with multi-scale satellite remote sensing. *Journal of Great Lakes Research*, *39*, 78–89.

Silva, T. S., Costa, M. P., Melack, J. M., & Novo, E. M. (2008). Remote sensing of aquatic vegetation: Theory and applications. *Environmental Monitoring and Assessment*, *140*(1–3), 131–145.

Stratoulias, D., Balzter, H., Zlinszky, A., & Tóth, V. R. (2015). Assessment of ecophysiology of lake shore reed vegetation based on chlorophyll fluorescence, field spectroscopy and hyperspectral airborne imagery. *Remote Sensing of Environment*, *157*, 72–84.

Swain, P. H., & King, R. C. (1973). Two effective feature selection criteria for multispectral remote sensing. *LARS Technical Reports. Paper 39, Technical Note 042673*.

de Tezanos Pinto, P., & O'Farrell, I. (2014). Regime shifts between free-floating plants and phytoplankton: A review. *Hydrobiologia*, *740*(1), 13–24.

Tian, Y. Q., Yu, Q., Zimmerman, M. J., Flint, S., & Waldron, M. C. (2010). Differentiating aquatic plant communities in a eutrophic river using hyperspectral and multispectral remote sensing. *Freshwater Biology*, *55*(8), 1658–1673.

Tomaselli, M., Gualmini, M., & Spettoli, O. (2000). *La vegetazione della Riserva Naturale delle Valli del Mincio.* Parma (IT): Collana Annali Facoltà di Scienze Matematiche Fisiche e Naturali dell'Università di Parma, 90.

Villa, P., Boschetti, M., Morse, J. L., & Politte, N. (2012). A multitemporal analysis of tsunami impact on coastal vegetation using remote sensing: A case study on Koh Phra Thong Island, Thailand. *Natural Hazards*, *64*(1), 667–689.

Villa, P., Bresciani, M., Braga, F., & Bolpagni, R. (2014b). Comparative assessment of broadband vegetation indices over aquatic vegetation. *Selected Topics in Applied Earth Observations and Remote Sensing, IEEE Journal of*, *7*(7), 3117–3127.

Villa, P., Duan, H., & Loiselle, S. A. (2015). *Using remote sensing to assess the impact of human activities on water quality: Case study of Lake Taihu.* China. In Advances in Watershed Science and Assessment: Springer International Publishing, 85–110.

Villa, P., Laini, A., Bresciani, M., & Bolpagni, R. (2013). A remote sensing approach to monitor the conservation status of lacustrine *Phragmites australis* beds. *Wetlands Ecology and Management*, *21*(6), 399–416.

Villa, P., Lechi, G., & Gomarasca, M. A. (2009). Multivariate differencing techniques for land cover change detection: The normalized difference reflectance approach. In P. G. P. P. Ho (Ed.), *Geoscience and remote sensing. 2009.* (pp. 277–300). Vienna: In-Tech.

Villa, P., Mousivand, A., & Bresciani, M. (2014a). Aquatic vegetation indices assessment through radiative transfer modeling and linear mixture simulation. *International Journal of Applied Earth Observation and Geoinformation*, *30*, 113–127.

Vis, C., Hudon, C., & Carignan, R. (2003). An evaluation of approaches used to determine the distribution and biomass of emergent and submerged aquatic macrophytes over large spatial scales. *Aquatic Botany*, *77*(3), 187–201.

Wang, L., Dronova, I., Gong, P., Yang, W., Li, Y., & Liu, Q. (2012). A new time series vegetation–water index of phenological–hydrological trait across species and functional types for Poyang Lake wetland ecosystem. *Remote Sensing of Environment*, *125*, 49–63.

Wardlow, B. D., & Egbert, S. L. (2008). Large-area crop mapping using time-series MODIS 250 m NDVI data: An assessment for the US Central Great Plains. *Remote Sensing of Environment*, *112*(3), 1096–1116.

Wetzel, R. G. (1992). Wetlands as metabolic gates. *Journal of Great Lakes Research*, *18*(4), 529–532.

Williams, D. J., Rybicki, N. B., Lombana, A. V., O'Brien, T. M., & Gomez, R. B. (2003). Preliminary investigation of submerged aquatic vegetation mapping using hyperspectral remote sensing. *Environmental Monitoring and Assessment*, *81*(1–3), 383–392.

Witten, I. H., & Frank, E. (2005). *Data mining: Practical machine learning tools and techniques.* Morgan Kaufmann.

Xie, Y., Sha, Z., & Yu, M. (2008). Remote sensing imagery in vegetation mapping: A review. *Journal of Plant Ecology*, *1*(1), 9–23.

Yang, J., Weisberg, P. J., & Bristow, N. A. (2012). Landsat remote sensing approaches for monitoring long-term tree cover dynamics in semi-arid woodlands: Comparison of vegetation indices and spectral mixture analysis. *Remote Sensing of Environment*, *119*, 62–71.

Zhao, D., Jiang, H., Yang, T., Cai, Y., Xu, D., & An, S. (2012). Remote sensing of aquatic vegetation distribution in Taihu Lake using an improved classification tree with modified thresholds. *Journal of Environmental Management*, *95*(1), 98–107.

Zlinszky, A. (2010). Measuring historic water levels of Lake Balaton and the neighbouring valleys. *Acta Geodaetica et Geophysica Hungarica*, *45*(1), 39–47.

Zlinszky, A., & Timár, G. (2013). Historic maps as a data source for socio-hydrology: A case study of the Lake Balaton wetland system, Hungary. *Hydrology and Earth System Sciences*, *17*(11), 4589–4606.

Zlinszky, A., Mücke, W., Lehner, H., Briese, C., & Pfeifer, N. (2012). Categorizing wetland vegetation by airborne laser scanning on lake Balaton and Kis-balaton, Hungary. *Remote Sensing*, *4*(6), 1617–1650.